Medizinische Fakultät
der
Universität Duisburg-Essen

Institut für Anatomie und
Medizinische Klinik II des Kath. Krankenhaus Philippusstift
Akademisches Lehrkrankenhaus der Universität Duisburg-Essen

Magnetocardiography in unshielded location in coronary artery disease detection using computerized classification of current density vectors maps

Inaugural–Disseration
Zur
Erlangung des Doktorgrades der Medizin
durch die Medizinische Fakultät
der Universität Duisburg-Essen

Vorlegt von
Illya Chaykovskyy
aus Kiew, Ukraine

2005

Dekan: Univ.-Prof. Dr.rer.nat. K.-H. Jöckel

1.Gutachter : Univ.-Prof. Prof. h.c. Dr. med. M.Blank

2.Gutachter: Univ.-Prof. Dr. med. R. Erbel

Tag der mündlichen Prüfung: 24.05. 2006

LIST OF ORIGINAL PUBLICATIONS

I. Chaikovsky I., Koehler J., Hecker T., Hailer B., Sosnitsky V., Fomin W.(2000):
High sensetivity of magnetocardiography in patients with coronary artery disease and normal or unspecifically changed electrocardiogram.
Circulation. 102 (Suppl.II). 3822.

II. Chaikovsky I., Steinberg F., Hailer B., Auth-Eisernitz S., Hecker T., Sosnitsky V., Budnik N., Fainzilberg L.(2000) :Possibilities of magnetocardiography in coronary artery disease detection in patients with normal or unspecifically changed ECG.
In: Lewis B., Halon D., Flugelman M., Touboul P.(Eds.): Coronary artery diseases: Prevention to intervention. P. 415-421.
Bologna:Monduzzi Editore

III.Chaikovsky I. , Primin M ., Nedayvoda I. , Vassylyev V , Sosnitsky V., Steinberg F.(2002): Computerized classification of patients with coronary artery disease but normal or unspecifically changed ECG and healthy volunteers. ´
In: Nowak H., Haueisen J., Giessler F., Huonker R. (Eds.) :Biomag 2002: Proceedings of the 13-th International Conference on Biomagnetism . P. 534-536.
Berlin :VDE Verlag

IV. Chaikovsky I., Katz D., Katz M.(2003):
Principles of magnetocardiographic maps classification and CAD detection.
International Journal of Bioelectromagnetism 5. 100-101.

V. Hailer B., Chaikovsky I., Auth-Eisernitz S., Shäfer H., Steinberg F., Grönenemeyer D.H.W.(2003):
Magnetocardiography in coronary artery disease with a new system in an unshielded setting.
Clin.Cardiol. 26. 465-471

VI. Vasetsky Y., Fainzilberg L., Chaikovsky I.(2004):
Methods of structure analysis of current distribution in conducting medium for magnetocardiography (in Russian) .
Electronic modeling. 26. 95-116.

VII.Hailer B., Chaikovsky I., Auth-Eisernitz S., Shäfer H., Van Leeuwen P.(2005):
The value of magnetocardiography in patients with and without relevant stenoses of the coronary arteries using an unshielded system.
PACE 28 . 8-15.

VIII. Chaikovsky I., Budnik M., Kozlovski V., Ryzenko T., Stadnjuk L., Voytovich I.(2005):
Supersensitive magnetocardiographic system for early identification and monitoring of heart diseases (medical application).
Control systems and computers. 3. 50-62.

CONTENTS Page

1. INTRODUCTION

1.1. History of magnetocardiography

Magnetocardiography is non-invasive and risk-free technique allowing body-surface recording of the magnetic fields generated by the electrical activity of the heart.

The difficulty in the recording of a recording of the magnetocardiogram is the weakness of the signal: magnetic field generated by currents flowing in the heart is in the order of 10^{-10} to 10^{-12} Tesla, which is much weaker than earth's magnetic field and urban noise (s. Figure 1).

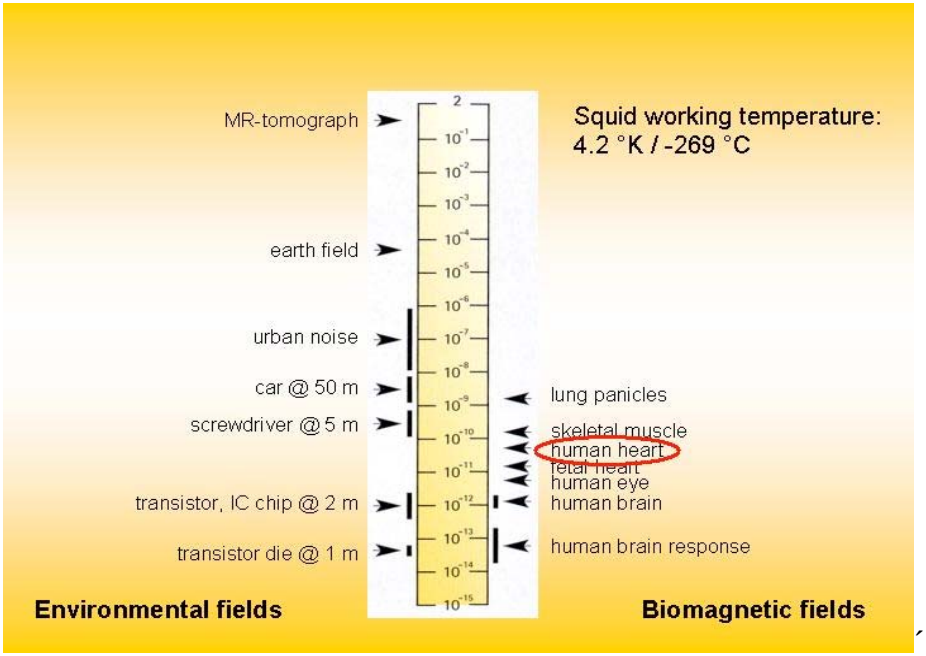

Figure 1: Scale of magnitudes of different magnetic field sources

The first magnetocardiogram was recorded by BALUE and McFEE (1963).

In the first recording of the human magnetocardiogram Balue and McFee used two coils, each made of several million turns of thin copper wires around a ferromagnetic core, kept

at room temperature. Measurements were done in a remote rural site, away from the urban electromagnetic noise. However, the sensitivity of used sensor was insufficient.

In the early 1970's technological progress allowed the use allowed the use of superconducting magnetometers. COHEN at al. (1970) first used SQUID magnetometer in a magnetically shielded room, to record a magnetocardiogram with an improved spatial accuracy and a higher spatial-to-noise ratio.

SQUID magnetometers are , in present, the only practical tool available for MCG recordings. In the 1970's the MCG studies by Cohen at al. significantly contributed to the initial methodology of MCG recordings, but should not be regarded as clinical research ,although physicians were occasionally involved. In the early1980's preliminary clinical research studies were conducted in Germany, USA, Finland, Japan , Italy. At that stage ,a single SQUID sensor was sequentially moved from point to point of the measurement grid in a plan near the anterior torso. First truly multi-channel system were developed in 1988-1990 (Siemens, Philips, BTI). All these system were designed to operate only in a well-shielding rooms (s. Figure 2).

Figure 2: Multi-channel MCG system (Phillips) installed in the shielded room

Using these systems as of mid –1990's several clinical studies were conducted in the above mentioned countries. At the same time some extremely inexpensive small unshielded MCG systems were developed and put into operation in Russia (Moscow) and Ukraine (Kiew) and later in Germany and USA. This kind of systems is able to work directly in the clinical setting without any shielding and, therefore, more practical for using in the clinical routine.

1.2 Electrophysiological basis of magnetocardiography

The de- and repolarisation of the cardiac muscle cell are based on ion currents through the cellular membrane , which are conditional upon a temporally different permeability for single ions. This causes changes in the membrane as well as corresponding intra and extra cellular volume currents. These volume currents spread in the body and cause potential differences on the body surface , which are again detectable as changes in the electrical potential with an electrocardiograph. Corresponding to the anatomic arrangment and function of the specialized cardiac conduction system of the heart , it is electrically exited from the basis to the apex. In a simplified way the electrical activity can be represented in the form of a current dipole (so-called equivalent current dipole). This electrical dipole is not only surrounded by an electrical field by also by a magnetic one. The spatial dispersion caused by a current dipole can be calculated according the Biot-Savart Law. The recording of the periodic changes in the magnetic field during the cardiac cycle is called magnetocardiogram.

1.3 Main differences between MCG and ECG

MCG has morphological feature similar to ECG: P-wave, QRS complex, T and U waves. Temporal relationship between them are also generally similar to ECG (SAARINEN at al.,1978).

All MCG systems provide measurement of the magnetic field components perpendicular (radial or z-component) to the anterior chest (Bz).

The main difference between spatial ECG and MCG patterns is the spatial angle of 90° between them (s. Figure 3).

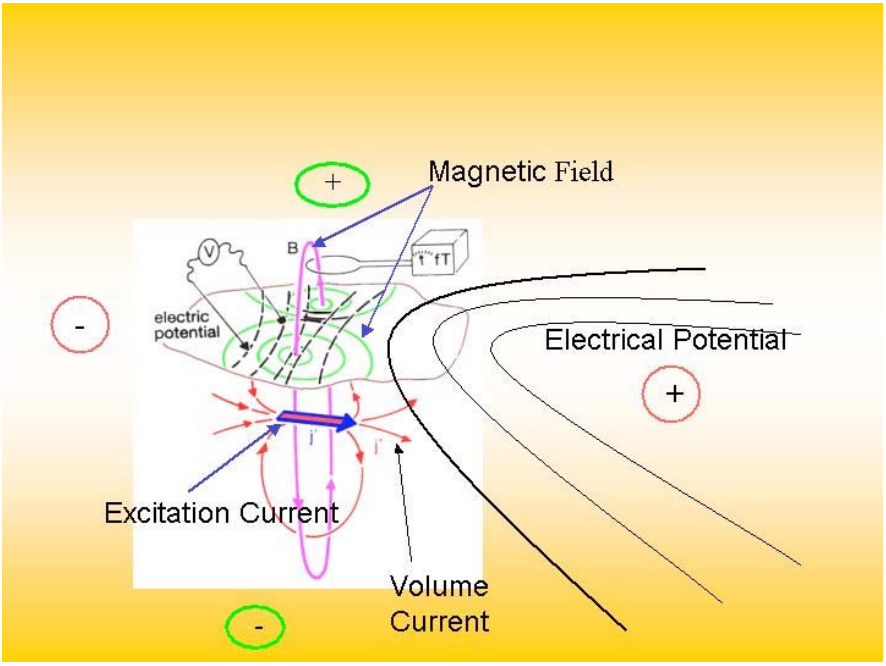

Figure 3: Spatial relationship between electrical and magnetic fields

MCG is most sensitive to currents tangential to the chest surface, whereas ECG is more sensitive to radial currents. Besides MCG is sensitive to closed (vortex) current sources, which do not cause any potential drops on the body surface and can not be detected by ECG as shown by KOCH (2001).

In addition MCG is affected less by conductivity variations in the body (lungs, muscles, skin) than ECG. MCG is fully noninvasive method , thus, the problems in the skin-

electrode contact are encountered in ECG are avoided. The ischemic diastolic TP shifts and "true" ST shifts can be distinguished from each other in direct-current MCG, since there are no potentials generated by the skin-electrode interface.

1.4 Clinical application of MCG

MCG has been applied mainly in the following clinical settings:

a) evaluation of the presence and localization of coronary artery disease;

b) evaluation of percutaneous coronary intervention results;

c) identification of viable myocardium after myocardial infarction;

d) risk stratifications in ischemic patients ;

e) evaluation of LV hypertrophy;

f) assessment of the evolution of the myocarditis;

g) early diagnosis of arrhytmogenic right ventricular dysplasia;

h) assessment of rejection reactions after heart transplantation;

i) fetal rhythm assessment;

j) localization of pre-excitation and other cardiac sources

1.5 Methods of clinical evaluation of MCC data

As MCG technology is much younger than the ECG and more closely related to modern methods of data processing not usually employed in ECG interpretation, a variety of methods and indicators for medical analysis available in the current stage of MCG development, must be evaluated in terms of its clinical relevance.

MCG analysis can be expressed at several levels of increasing complexity of magnetocardiographic signal transformation.

Level 1: The first level of analysis is similar to routine morphological analysis of the 12 – lead ECG. Since amplitude- time MCG curves look like the ECG (s. Figure 4) and both have the same nomenclature of waves and intervals they can be used similarly for the definition of cardiac hypertrophy (KATAYAMA at al. 1989, 1990) and myocardial infarction (MURAKAMI at al., 1987).

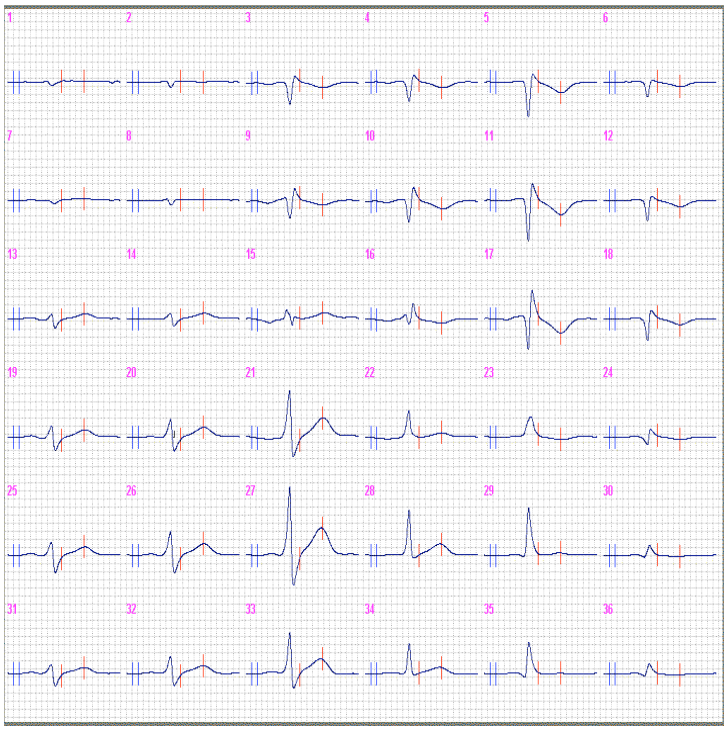

Figure: 36 averaged magnetocardiographic curves

Level 2: The second level is a spectro-temporal analysis. The relative power of a cardiac signal for various frequency bands and their spectral variability and time-domain analysis (such as QRS duration) of the MCG can be provided at specific measurement points . An example in the ECG analog of this approach is the well known analysis of ventricular late potentials.

Here, the diagnostic purpose of the MCG analysis could be to estimate ventricular depolarization inhomogeneity in order to assess the risk of arrhythmia occurrence. This

approach has been employed, for example, by ACHENBACH et al.(1995) to estimate the risk of graft rejection .

Level 3: Here the 36 measurement points of the MCG-7 are summarised in an averaged curve. Such an approach provides a more generalized representation of myocardial excitation. For example, the areas under the P-wave or the QRS-complex reflect overall " electrical energy" generated due to excitation of atria and ventricles. BOBROV et al.(1997) suggest that the ratio of these magnitudes may relate to the degree of cardiac failure .

OJA et al.(1995) employing a specially devised magnetocardiograph to construct 3 orthogonal components, have presented a vectorcardiographic display in which they could estimate the amplitude values of x-, y-, and z-components during the P-wave, QRS-complex and ST-T interval, the amplitude and direction of the spatial maximal QRS-vector and QRS-vector duration for the diagnosis of myocardial infarction .

All these analysis methods follow customary ECG-procedures and according to most authors have a sensitivity and specificity approximately equal to the conventional electrocardiographic methods. However, the information contained in the MCG for exceeds these interpretations, as will be demonstrated in the next 4 levels.

Level 4: Magnetic field mapping. This requires the construction of maps showing the distribution of the magnetic field obtained at specific measurement points and precise moments of the cardiac cycle. These maps are constructed along the principles of geographical or meteorological maps. Areas with identical value of given parameter are color coded. Each map then reflects the average of all measurement points. At a given point, such interpretation of electrical activity of the heart provides a number of essential advantages. First of all, with the help of interpolation methods, all valuable data, including those situated between the points of the measuring grid are taken into consideration.

Secondly, such maps actually reflect the natural projection of electromagnetic phenomena registered above the thorax surface of different parts of the heart.

The two most important characteristics of a magnetic field map are : 1) the number of magnetic field extrema (in the physical meaning, local extrema of a magnetic field are points with maximal value compared to the surrounding magnetic field), in other words — the inhomogeneity of the map. 2) Mutual arrangements of these extrema.

As the main characteristic of such a map is reflected in the simultaneous location of magnetic field minima and maxima (the extrema of magnetic field) one can find the orientation of the equivalent current dipole (i.e. excitation wavefront) by drawing a line from a minimum to a maximum and turning this line counter-clockwise by 90 degrees (s. Figure 5).

On these principles, such maps are usually visually analyzed at one or several characteristic time points of the cycle, for example at QRS-onset, at R-max, QRS-offset, T-onset, T-max or T-offset (NOMURA at al.,1989, BROCKMEIER at al ,1997). They can also be made during the entire ventricular repolarisation period to detect myocardial ischemia as shown by CREMER at al.(1999), CHAIKOVSKY at al (2000). The main finding is that normal cardiac maps demonstrate a clear dipole structure (one minimum and one maximum). In contrast, maps of patients with ischemia due to coronary artery disease show additional non-dipole compartments. LANT at al. (1991) investigated time integral maps during the entire QRS-complex and/or ST-T interval .

The initial qualitative visual analysis method of magnetic field maps is sufficient to give a general impression of the main features of the electrophysiological (ab)normalities in the myocardium. Again, this is not sufficient for a quantitative description of specific features and does not allow for statistical analysis or separation of different cardiac disorders.

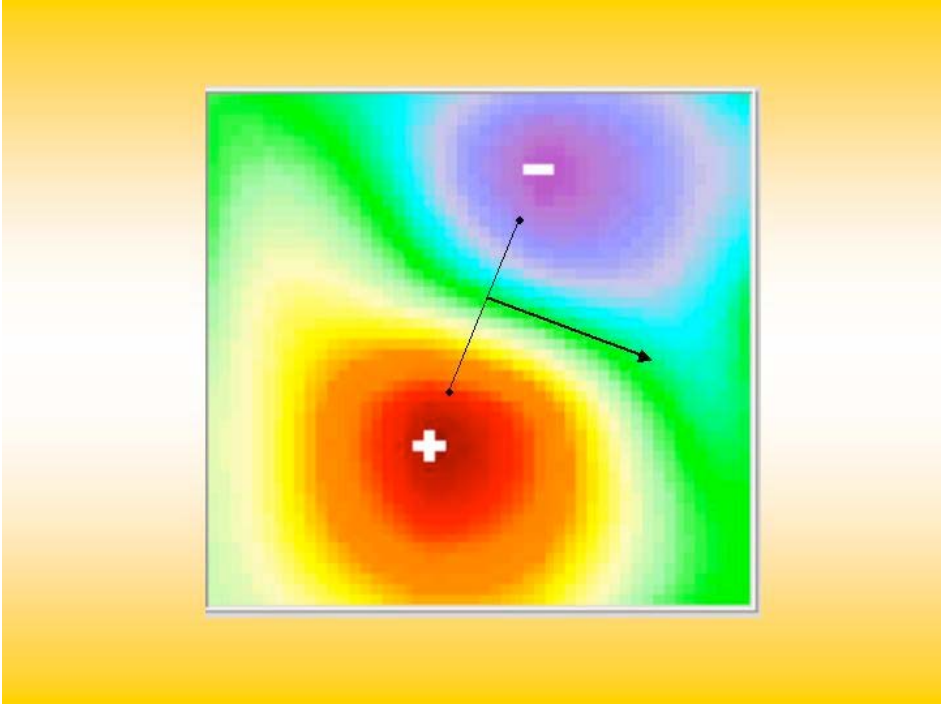

Figure 5: Magnetic field distribution map in the middle of ST-T interval. Arrow reflects orientation of equivalent current dipole

Level 5: Quantitative criteria of magnetic field evaluation.

The simplest approach here is to calculate the number of extrema in each map during a certain period of the cardiac cycle. The relative smoothness index, representing the sum of correlation factors between four sequential maps at the beginning of ST-segment has been proposed by GAPELJUK at al.(1998). In addition, there is the criterion based on estimation of complexity of extrema trajectories during ventricular excitation (STROINK at al., 1999).

KATZ and al. (2003) used classification of magnetic field maps, mainly based on the ratio of the greatest positive to the greatest negative extreme values for detecting of myocardial ischemia in patients with stenosis of LAD.

Another quantitative criterion, which was used for chronic and acute myocardial ischemia detection, is the variability of the ratio of the greatest positive to the greatest negative extreme values as well as variability of distance between them during the ST-T

interval, (PARK at al., 2005, STEINBERG at al., 2005). It is also known as the homogeneity coefficient for the integral estimaion of extreme numbers and their steepness during the ST-T interval (BOBROV at al., 2000). Another rather interesting approach consists of a spatial transformation (KLM-transformation) of the magnetic field distribution maps and calculation of the non-dipolar contributions to each map. ADAMS at al. (1998) used this method for myocardial ischemia assessment .

Further quantitative parameters have been suggested. GÖDDE et al. (2001) have, next to traditional maps of the magnetic field distribution, made quantitative maps which represent the spatial distribution of the fragmentation of a QRS-complex at each point of the measuring grid. It increases accuracy in the detection of the origin of ventricular tachycardia. The spatial distribution of the QT interval and its duration coupled with some smoothness indices are shown in the studies of HAILER et al. (1998, 1999).

Another approach at this level might be considered as a statistical one (CHAIKOVSKY at al., 2002). The steps of this method are as follows:

The collection of a representative learning group consisting of healthy volunteers and well -documented patients.

The description of every map of each patient by set of specific numerical parameters (more than 50 parameters reflecting the homogeneity of ventricular repolarization and spatial – time distribution of the magnetic field within the ST-T interval for every map). This will provide a large parameter matrix for the entire learning population.

The development of classification algorithms based on methods of multivariate statistics – stepwise discriminant analysis (forward stepwise). The main advantage of this method is the selection of the most informative criteria and the formulation of a classification rule consisting of a rather small number of parameters (perhaps no more than 10).

A check of the robustness of such a classification algorithm by mathematical methods (cross-validation, "pessimistic" forecast). The validation of classification rules developed through “blind” testing of various groups.

This method would finally allow for a completely computerised and statistically correct classification of patients which then could be applied to different diagnostic tasks.

Similar method was used by MORQUET at al.(2002) for assessment of myocardial viability.

The purpose of all these various indexes is the same - to provide a quantitative inhomogeneity estimation of magnetic field distribution maps and therefore - to some extent - of the source(s) which produce this field.

Definition of the inverse problem solution:

More immediate and physiologically correct information could be deduced from the MCG analysis on the basis of the inverse electrodynamics problem solution. This term means the reconstruction of electrical events in the heart on the basis of recordings carried out above the surface of the human body. As in the MCG the magnetic field is measured not on the actual surface of the body, but above it, it is recorded in a measurement plane at a small distance from the skin covering the chestcage.

Modeling of inverse problem is rather complicated and solution might be ill-posed (HAMALAINEN and NENONEN , 1999).

However, the conductivity of different tissues and the shape of the body cage have less influence on the MCG then on the ECG. Also the spatial resolution of the MCG is much higher. Therefore the magnetocardiogram does make a more precise solution of the inverse problem possible.

The “further on the dimensions of the excitation area, the volume of the acute cardiac tissue, the distance inverse” solution purports to bring a functional relationship

between the measured magnetic field and the reconstructed sources. It all depends on which model is chosen, a punctual dipole, the current layer distributed in a plane or current distributed in a volume.

The proper choice of the source model depends from the sensor, the diameter of the magnetic flux transformation coil as well as on the (patho)physiologic characteristics of the process c.q. the disorder under investigation. It would appear therefore that different models of the “inverse” solution will be most suitable for different clinical tasks.

Level 6: The representation of all electrical sources as one equivalent dipole.

Here it is assumed that all electrical activity of the heart originates from one point. While this does not mean, that the heart is actually a point source, the results of its activity on the body surface are considered to be equivalent to effects, which would be observed there if there were one point source. Such representation of one source serves also as the conceptual basis for vector-cardiography. It is evident, however, that this does not allow for separate activities of the various parts of the heart which the MCG purports to be able to do.

The determination of the point source position at the moment of an ectopic QRS-complex beginning has been used to localize the site of ventricular arrhythmia origin or the detection of the delta-wave - for the localization of accessory activation pathways (MOSHAGE, 1996). The strength of the effective dipole at the R-maximum point and S-minimum point has also been employed as a criterion for the estimation of risk of graft rejection after cardiac transplantation (SMITZ at al., 1992). VAN LEEUWEN at al.(1997) has proposed its orientation in a frontal plane at characteristic moments of the cycle as a criterion for ischemia detection . The shape of curves of dipole orientation and strength during the QRS interval is generally considered a sensitive marker for MI. CHAYKOVSKY et al.(1999) have analyzed curves of equivalent dipole depths during

ventricular excitation, i.e. the character of dipole movement in a frontal-backward direction. To a certain extent this reflects the source distribution in the sagittal plane. In fact, this plane remains outside of the analysis, because the MCG is usually registered in the frontal plane only. This analysis appeared to be rather informative for the diagnosis of MI, including non-Q wave MI .

The correlation between the instantaneous current dipole and its localization in consecutive heart beats (so-called “electrical circulation) was proposed for assessment of myocarditis evolution (AGRAVAL at al.,2000) .

Level 7. Data representation on the basis of 2-D current density distribution maps.

The analysis of current density distribution maps gives additional options. Up to now, there are only very few publications using this kind of analysis (LEDER at al., 1998; PESOLA at al.,1999 , CHAIKOVSKY at al., 2000). As a main diagnostical criteria remains homogeneity of the maps and direction of current density vectors. It is important to note that this level of analysis is unique for the MCG and has no analogue in ECG diagnostics. The main reason for this is that an inverse solution based on the registration of potentials on the body surface is a highly complicated affair as a precise definition of coordinates for every electrode would be required. Another reason is that the influence of the conductivity differences of the tissues surrounding the heart (which is different for every individual patient) is much larger on ECG electrodes than for magnetocardiographic signals. Also an inverse solution based on registration of potentials does not allow for the measurement of elementary local sources, in contrast to the inverse solution based on the magnetic field. Such a current density distribution map is presented in Figure 6. This image reflects the motion of electrical charges inside the heart, where the length and magnitude of the arrows reflect the density of these charges. Black and short arrows reflect the lowest values, the red and longest the highest, blue being in the middle. Flow–chart for

visual map classification within the ST-T interval was developed by us and used for myocardial ischemia detection (CHAIKOVSKY at al, 2003; HAILER at al.,2003, 2005). The classification is mainly based on the dipolar or nondipolar structure of the map and the direction of the main current density vectors. The symmetry or asymmetry of the served for further specification.

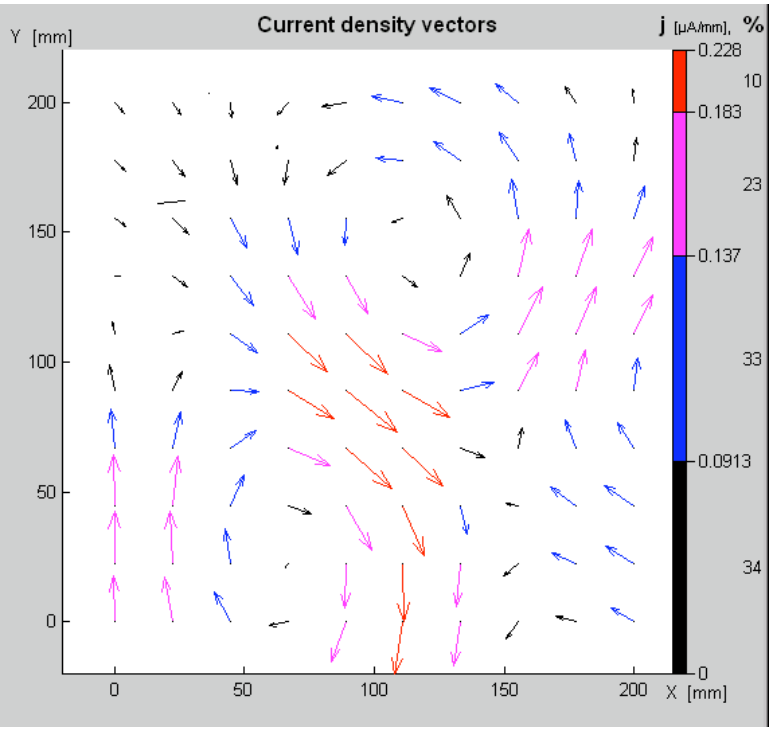

Figure 6: Current density distribution map in the middle of ST-T interval

While this proposed scoring system depends to some degree on the experience of the observer, after some training the procedure is not time-consuming. Objective, computerized classification of CDV maps is still pending in the literature.

Level 8: Analysis of 3-D source distribution providing magnetocardiographic tomography (similar to MRI or CT).

The first examples of this data representation are shown in Figures 7and 8. Figure 7 represents a 3-D distribution of magnetic dipoles density . “Clouds” of these dipoles represent the excited zones of the myocardium at certain time moments of the cardiac cycle

(PRIMIN at al., 2003). Next step might be a tomographic, layer by layer, reconstruction (s. Figure 8).

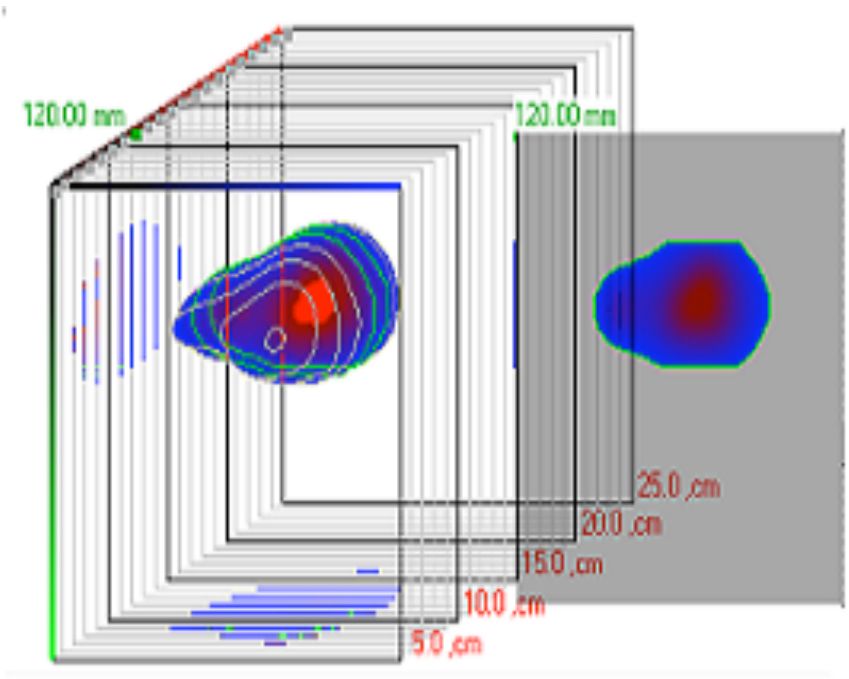

Figure 7: 3-D dipoles density reconstruction at the middle of ST-T interval Axonometric projection of cube of current reconstruction with "cloud" of dipoles density. Layers with maximal density of upper currents area (right) and lower currents area are marked

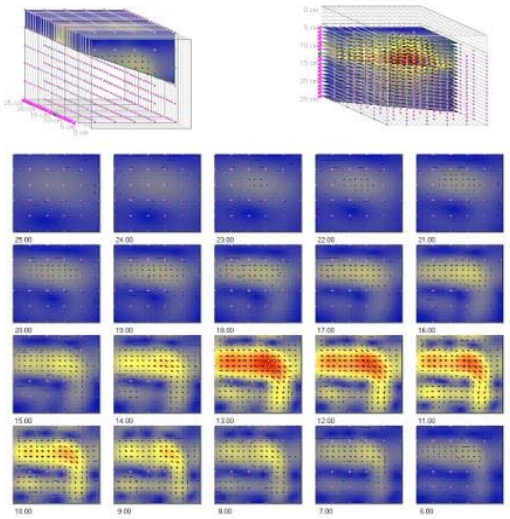

Figure 8: 3-d current reconstruction at the middle of ST-T interval

Upper row: axonometric projection of cube of current reconstruction- frontal view (left) and sagittal view (right)

Low rows: Current density vectors maps on different distance from plane of measurement(from 6 to 25 cm)

If density and the co-ordinates of all magnetic dipoles are known, current density maps could be obtained for any layer distant at various depths from the measurement plane.

This kind of analysis could provide additional anatomically related-information.

Rather close approach was demonstrated by MAKELA at al. (2003) , in which current distributions were superimposed on magnetic resonance images. Homogeneity of current distribution was evaluated.

1.6 Aims of the study

The study reported in this thesis was designed to investigate detection of myocardial ischemia in a heterogeneous CAD population including subsets of patients with ischemia in any of the main coronary artery branches regions but without prior myocardial infarction and with normal 12-leads ECG at rest by magnetocardiography at rest.

The specific aims were :

1. To study the capability of simple magnetocardiographic system , installed in unshielded location in a clinical setting.
2. To develop an objective computerized classification of the current density distribution maps within ST-T interval and study the value of this classification system to detect myocardial ischemia.

2. MATERIALS AND METHODS

2.1. Study subjects

Subjects of the study were included over a period from December 1999 until November 2002. MCG recordings were taken using a stationary system, installed in a division of cardiology (Department of Medicine II, Phillipusstift, Essen, Germany).

A total of 110 patients with CAD and 98 healthy controls were included in the study. In further 2 subjects in CAD group and one subject in control group were excluded as a result of poor quality of the MCG signal that did not allow to determine the events (J-point, T-offset) of the cardiac cycle.

2.1.1 Patients with CAD

The patients were selected consecutively from all patients admitted to the hospital over a period of 1 year with the indication to coronary angiography due to chest pain.. Subjects with narrowing of the coronary arteries ≥ 50% in ≥ 1 vessel and no prior myocardial infarction or wall motion disturbances at rest were assigned to the CAD group. Patients excluded from the study were those with atrial fibrillation or atrial flutter, bundle- brunch block , abnormal Q-waves or ST depression/elevation in 12 lead ECG , pacemaker therapy, left ventricular hypertrophy as assessed by echocardiography, valvular heart disease , renal insufficiency with need for dialysis or other catabolic disease.

All patients were clinically stable during the study. All patients gave their written informed consent.

2.1.2 Control group

The control group consisted of 97 healthy subjects with no history of any cardiovascular disease, normal ECG at rest stress as well as normal echocardiogram at rest. The were mainly recruited from the local fire and police department.

Another 15 volunteers with no history of any cardiovascular disease were used for run-to-run and day-to-day reproducibility assessment . They were recruited from the employee of the hospital and company SQUID AG.

Baseline characteristic of all subjects are given in Table I.

Table I: Baseline subjects characteristics.

	Patients with CAD n = 108	Control group n = 97	Group for reproducibility assessment n = 15
Male	82	71	11
age (years)	61 ± 10	51 ± 8	40 ± 9
coronary status			
1-vessel	37		
2-vessel	37		
3-vessel	34		
ß-Blocker therapy	99		
ACE- Inhibitor	51		
Hypertension	71		
Diabetes mellitus	6		
High blood holesterol	48		
Familiar history for CAD	37		

2.2 MCG recordings and data processing

In all patients MCG were performed in close time relationship (24-48 hours) prior to coronary angiography.

All volunteers had MCG recordings in the morning time. In 15 volunteers served for reproducibility assessment second recording was done in a separate session later that day, which included repositioning and MCG recording. The third recording in this group was done next day, in about 24-30 hours after baseline MCG recording.

The magnetocardiography recordings were performed with a four-channel SQUID biomagnetometer (s. Figure 9).

Figure 9: Four-channel magnetocardiograph (SQUID AG, Essen) in unshielded setting

The sensing coils were 20 mm in diameter and each channel was configured as a 2nd order gradiometer with a 6 cm baseline(s. Figure 10).

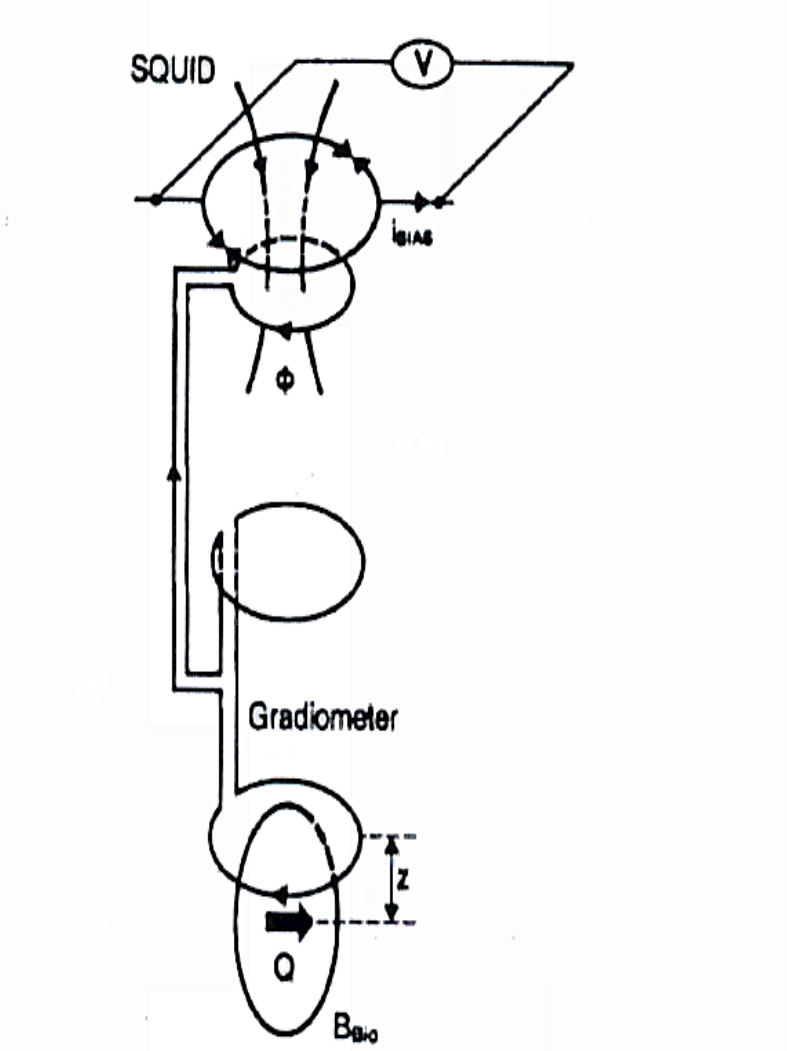

Figure 10: Sketch drawing of the gradiometer antenna system 2nd order coupled to the SQUID sensor

The channels are on 2 by 2 grid. System noise was characteristically less < 25fT/√Hz for frequencies > 1 Hz. The system was installed in an unshielded clinical setting and during normal daytime operation , environmental noise was relatively constant. During acquisition, power lines represent the most dominant source of high amplitude noise (s.Figure 11 A).

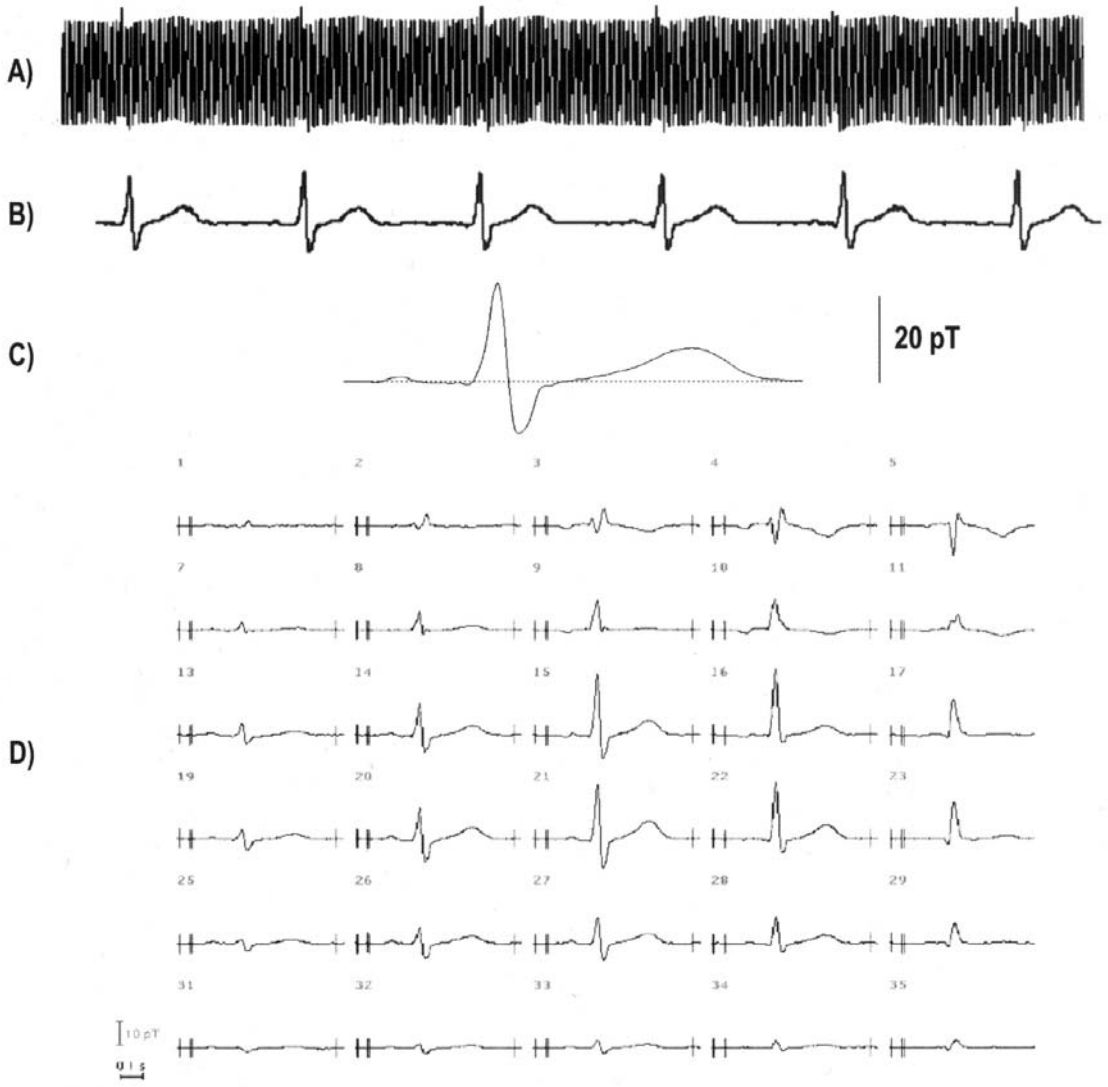

Figure 11: Example of MCG signals.
(A) Raw data in channel 21 with power line noise.
(B) Same channel : 50 Hz notch filtered data.
(C) Same channel : averaged signal , DC offset corrected prior to the P-wave.
(D) Averaged signal in at all 36 registration sites.

Subjects were examined in a supine position. MCG recordings were obtained at nine prethoracic sites within a 6 by 6 rectangular grid with a 4 cm pitch over the precordial area. The sensor was positioned as close to the thorax as possible, directly over the heart , initially at the jugulum (s. Figure 12).

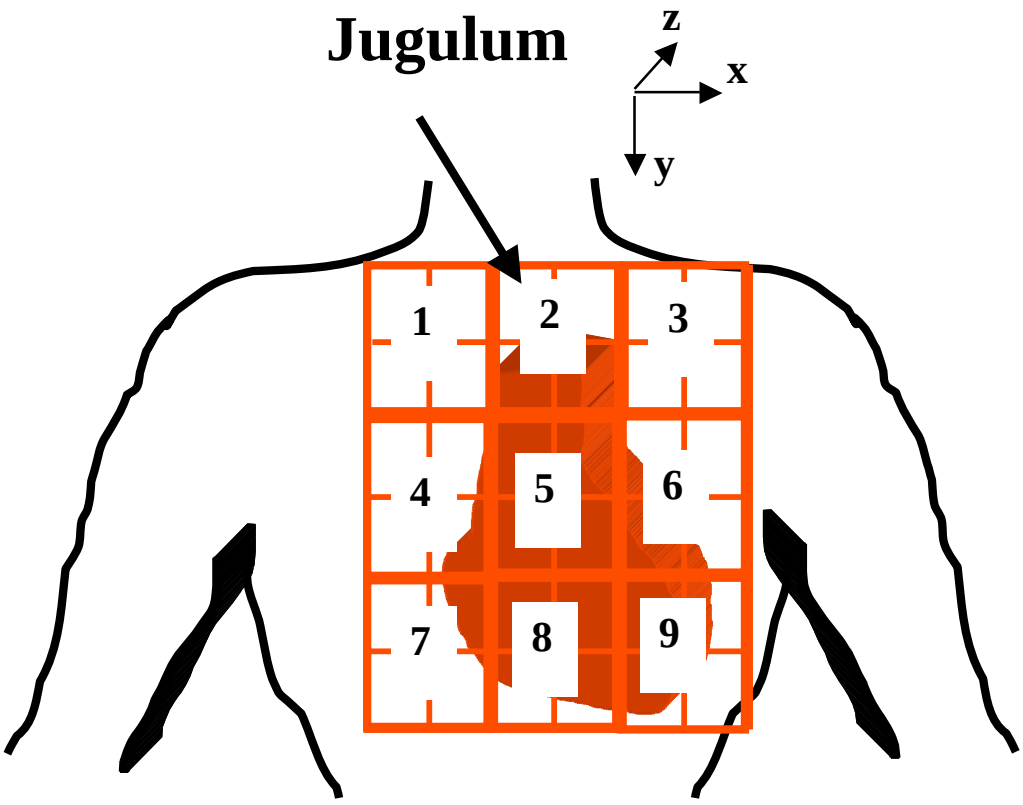

Figure 12 : 6 by 6 rectangular grid used for MCG registration, the covered precordial area is 20 by 20 cm. The sensor was positioned initially above the jugulum

The examination table with the patient resting in a stable position was then moved systematically to each of the nine predetermined position under the SQUID detector.

Data were recorded at each registration site for 30 second at a sampling rate of 1 kHz while implementing a 0.1-120 bandpass filter. Simultaneously , lead II of the surface ECG was registered. All data were stored on hard disk for further evaluation. The total time for each measurement was about 10 minutes.

2.3.MCG analysis

The MCG signal of each subject was notch filtered to eliminate power line frequencies (s. Figure 11 B).

The single beats were identified on the basis of the R-peak in the lead II ECG and at each the MCG recording site the beat were averaged. The averaged beats were then DC offset corrected with respect to a short signal interval in the TP interval immediately prior to the P-wave (s. Figure 11 C). For further analysis current density vector (CDV) maps were reconstructed. The calculation of these maps is based on inverse solution (ROMANOVITCH, 1997). The CDV maps reflect the complex source structure associated with distributed excitation wavefronts within the heart. From the magnetic field values detected at each of the 36 registration sites the cardiac repolarization process was projected onto a plan containing 100 points (s. Figure 6). At each point , the lead fields were shown as vector magnitudes indicating the strength and direction of the field. These 100 vector magnitude were calculated for each of 20 planes , each 20 by 20 cm , the top plane at the level of the sensor and the remaining 19 planes below the sensor , separated by 1 cm. Of the 20 planes , the plane chosen for further analysis was the one demonstrating the most coherence based on the minimum norm estimation. For each subject , CDV maps were generated every 10 ms within ST-T interval starting with the J-point to the end of the T-wave (s. Figure 14) for a total of ca. 20 maps.

For timing purposes lead II of the surface ECG served as reference channel. T end was defined visually as the point where T-wave returned to the TP baseline. Each CDV map in course of ST-T interval was analyzed automatically by means of a classification system with a scale from 0 (normal) to 4 (grossly abnormal) .

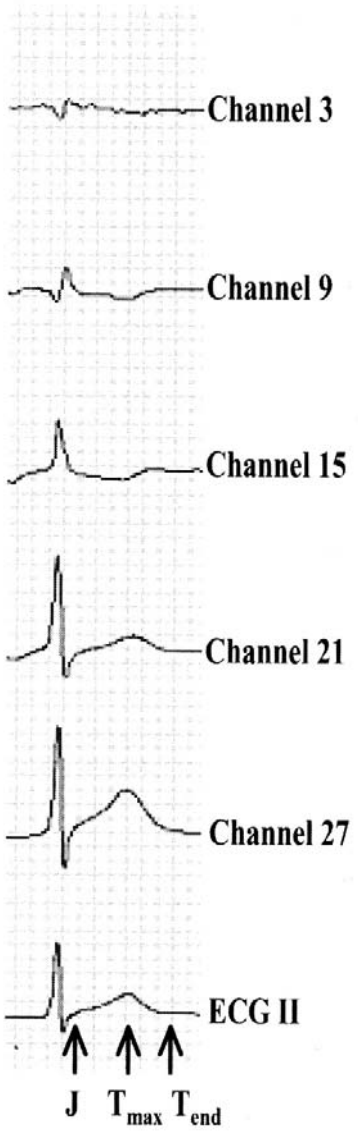

Figure 13: Example of MCG signals in various channels and corresponding ECG signal with marked referent points of ST-T interval

All steps of data acquisition and analysis were performed by the original software package MagWin (s. Figure 14). This package contains a common database as a central part, which stores patient informations, raw MCG and ECG signals, averaged cardiac cycles, magnetic and CDV maps, as well as results of maps classification. Each subsystem of the MagWin system is able to retrieve necessary input data directly from the database and save output data directly to the database.

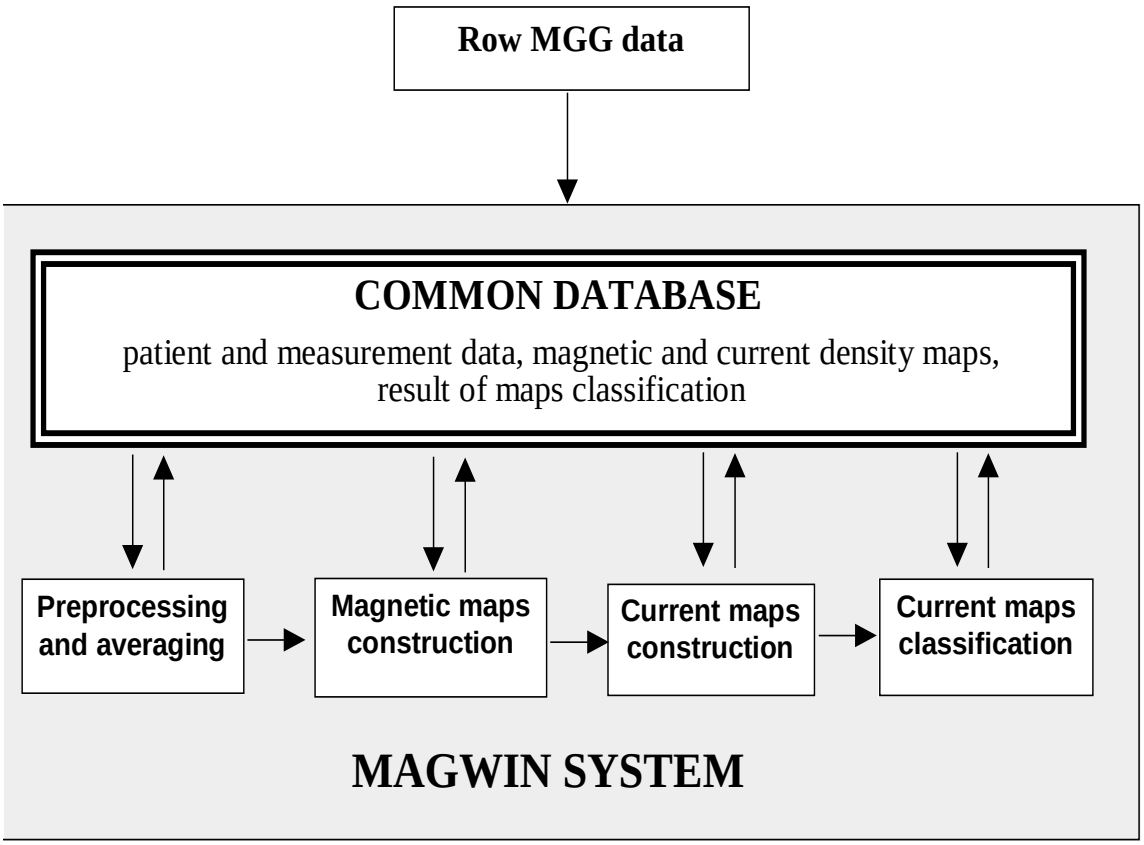

Figure 14: Principal scheme of software package MAGWIN

2.3.1. Models of current distribution

The maps classification is based on the following models.

The electrical generator during repolarization can be formulated as an extended current source located in the borderzone separating excited and non-excited zones of myocardium. In case of normal ventricular repolarisation, this excitation wavefront, integrated in a medium with homogeneous conductivity, should be directed left-downwards within a sector of $10–80^0$. Two types of currents are represented by this model: the so–called

“impressed currents“, due to the transmembraneous potential gradient and passive volume currents, generated by “impressed” currents (TRIP, 1983). Three different variants of current distribution are presented on Figure 15a,b,c. Green arrows display the impressed currents , concentric-oriented curves represent current lines of the “volume” currents. In the case of homogeneous conductivity these volume currents constitute two vortices, which are symmetrical and equal. The resulting map has an “ideal” dipolar structure (s. Figure 15 A) with only one area of respectively larger vectors directed left – downwards.

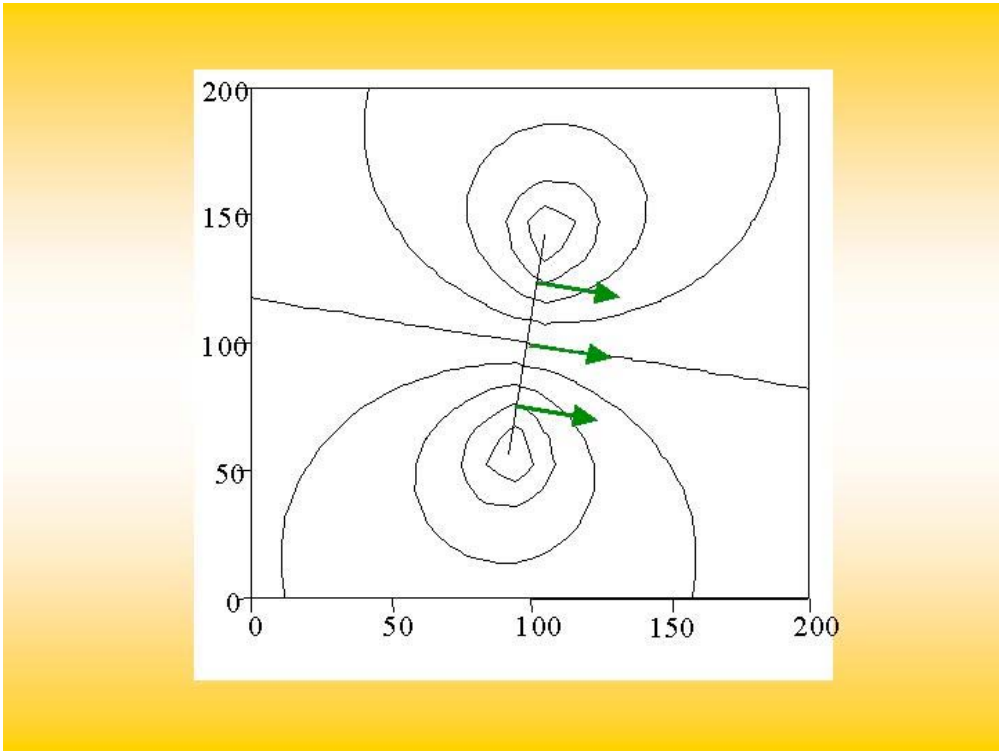

Figure 15 A: Model of current distribution:
One excitation wave-front in a medium with homogeneous conductivity

Appearance of inhomogeneity of conductivity due to some pathophysiological processes in the myocardium results in asymmetry and deformation of the vortexes (s. Figure 15 B), hence smaller portion of current vectors will be directed left-downwards.

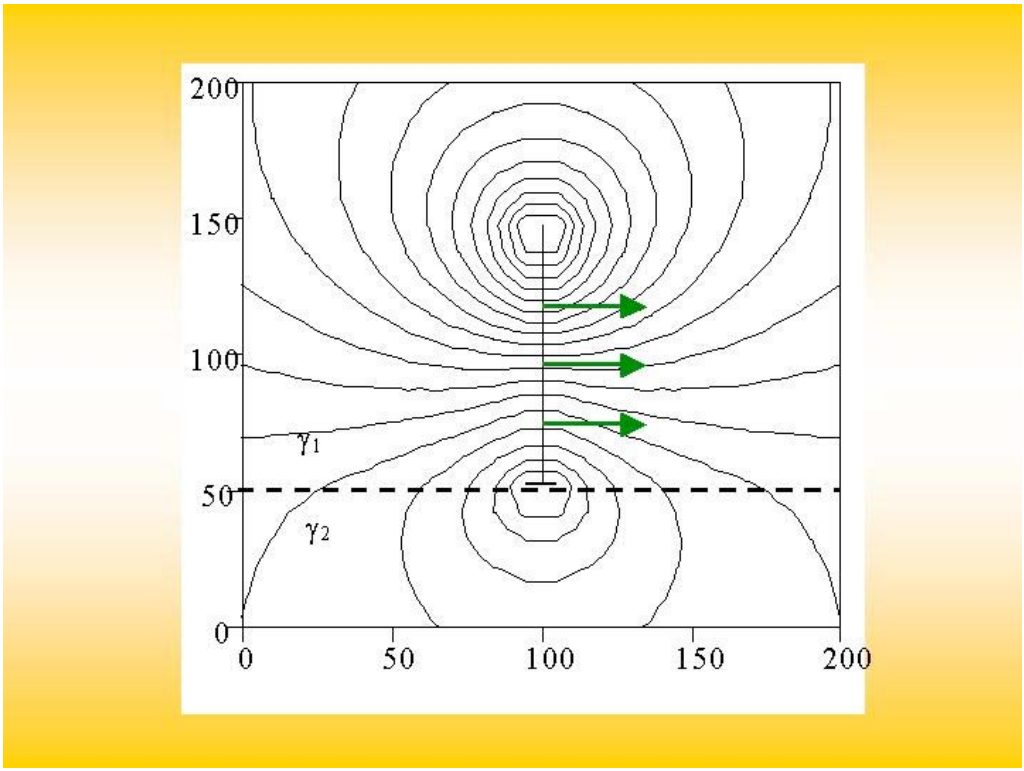

Figure 15 B: Model of current distribution:
One excitation wave-front in a medium with inhomogeneous conductivity
(two zones with a ratio of conductivities $\gamma_2/\gamma_1=1/3$)

The further increase of abnormality , as in case of ischemia , results in additional excitation wavefronts appearance. These pathological wavefronts will lead to a non-dipolar structure of the maps (s.Figure 15 C). In other words additional areas (clusters) of current vectors will appear. In most cases these areas will not be directed left-downwards , therefore portion of vectors directed to normal direction will further decrease.

However in some cases additional vector areas might be also directed left – downwards. Nevertheless these sort of maps should be defined as abnormal as well because of homogeneity decrease i.e appearance of additional areas (clusters).

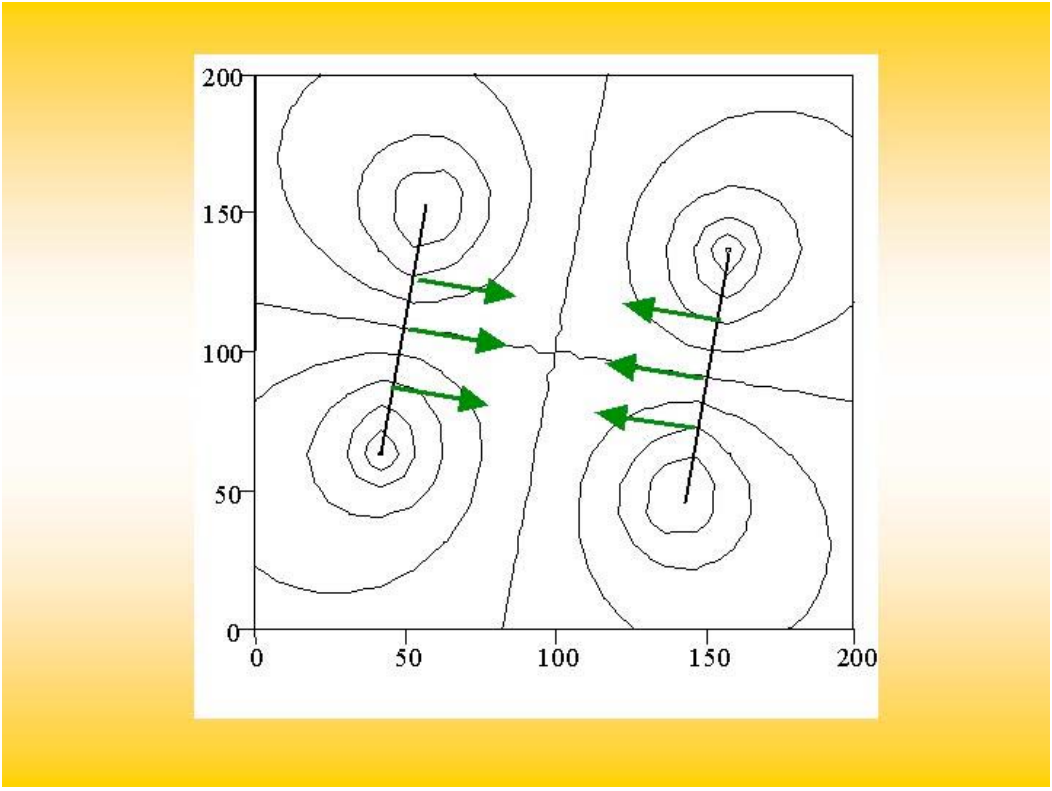

Figure 15 C: Model of current distribution:
Two excitation wave-fronts of equal strength and opposite direction

Based on this model classification scale from 0 to 4 with increasing abnormality is developed. The total length of current vectors directed left-downward determines the classification scale beside the presence of additional clusters.

2.3.2. Algorithm of computerized maps classification

Input of the algorithm is a $N*N$ matrix (N = 10) of current density vectors. Each vector is described by two parameters: x – horizontal projection, y – vertical projection. Using this information, the length (module) l and direction a in the range [0, 2π] of each vector are calculated by formulas:

$$l = \sqrt{x^2 + y^2}\ ,$$

$$a = \begin{cases} arctg(y/x), & if\ x > 0\ and\ y \geq 0; \\ arctg(y/x) + 2\pi, & if\ x > 0\ and\ y < 0; \\ arctg(y/x) + \pi, & if\ x < 0; \\ \frac{\pi}{2}, & if\ x = 0, y > 0; \\ \frac{3\pi}{2}, & if\ x = 0, y < 0. \end{cases}$$

Algorithm output is a number from “0” to “4” called map class. Map class qualitatively characterizes the analyzed map: “0” as the best class, “4” as the worst. The algorithm determines the direction of each vector in between a specified angle range (sector). Angle ranges may be presented by the so-called round chart (s. Figure 16).

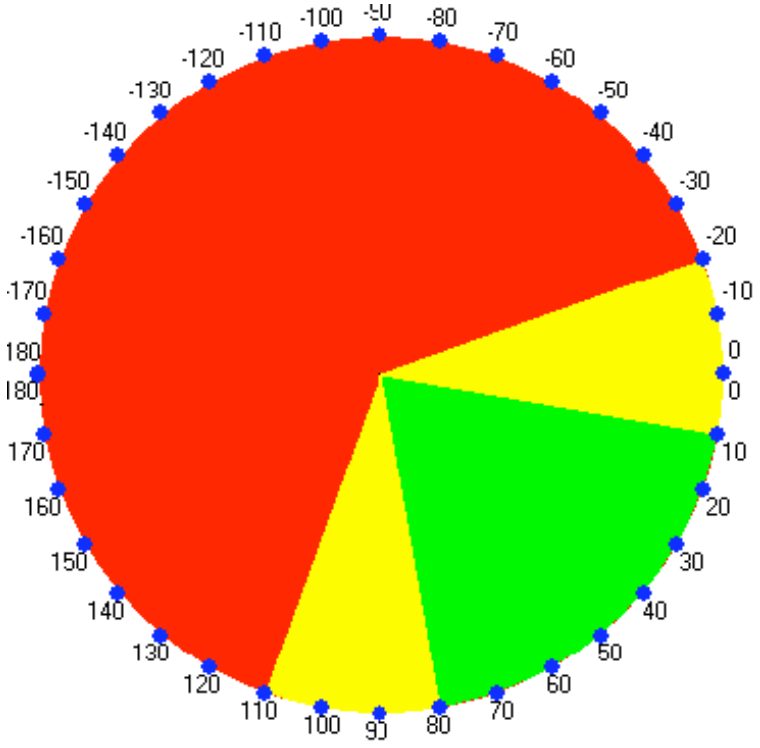

Figure 16: Vectors direction round chart: 3 types of sectors are marked

The round chart has 3 types of sectors: “G” – good (colored in green) , “Y” - marginal (colored in yellow), “R” – bad (colored in red). In order to simplify the

classification process all boundary values are automatically recalculated from degrees in the range of [-180, +180] into radians in the range of [-π, +π] and are furthermore transformed into ordered value formulas:

$$\chi_r = \chi_d \times \frac{\pi}{180}$$

$$\chi^* = \begin{cases} \chi_r, if\ \chi_r \geq 0; \\ \chi_r + 2\pi, if\ \chi_r < 0. \end{cases}$$

Therefore all transformed values of the thresholds are arranged and satisfy the following condition:

$$0 \leq R_2^* \leq G_1^* \leq G_2^* \leq R_1^*$$

To determine the sector to which the respective vector belongs the so-called indication of direction b is used. It is calculated by the following formula:

$$b_{i,j} = \begin{cases} G, if\ G_1^* \leq a_{i,j}^* \leq G_2^*; \\ Y, if\ G_2^* < a_{i,j}^* < R_1^*\ or\ R_2^* < a_{i,j}^* < G_1^*; \\ R, if\ a_{i,j}^* \leq R_2^*\ or\ R_1^* \leq a_{i,j}^*. \end{cases}$$

where a_{ij}^* is the value of the vector's direction transformed from the original value of the a_{ij} by formula:

$$a_{i,j}^* = \begin{cases} a_{i,j}, if\ a_{i,j} \geq R_2^*; \\ a_{i,j} + 2\pi, if\ a_{i,j} < R_2^*. \end{cases}$$

The algorithm selects all vectors having length greater than given length l0. Value of l0 is determined by formula:

$$l_0 = (\max_{i,j=1}^{10} l_{i,j}) \times p_0,$$

where l_{ij} is the length of vector located in the i-column and j-th row of the given map, p_0 is the given threshold. Then the following parameter is calculated:

$$\lambda = \frac{N_{GY}}{N_{ALL}},$$

where N_{GY} is the sum of length of the selected vectors with directions corresponding to *G* or *Y* sectors (good directions) of the round chart (that is having indication of direction $b_{i,j} = G$ or $b_{i,j} = Y$), N_{ALL} is the sum of length of all selected vectors:

$$N_{ALL} = \sum_{i=1}^{10} \sum_{j=1}^{10} l_{i,j} \times n_{i,j},$$

where

$$n_{i,j} = \begin{cases} 1, if\ l_{i,j} \geq l_0; \\ 0, if\ l_{i,j} < l_0. \end{cases}$$

To calculate N_{GY} value, following formula is used:

$$N_{GY} = \sum_{i=1}^{10} \sum_{j=1}^{10} l_{i,j} \times k_{i,j} \times n_{i,j},$$

where $k_{i,j}$ are *weights* calculated by formula:

$$k_{i,j} = \begin{cases} 1, if\ b_{i,j} = G; \\ 0, if\ b_{i,j} = R; \\ \left| (a_{i,j}^{*} - R_2^{*}) / (G_1^{*} - R_2^{*}) \right|, if\ b_{i,j} = Y\ and\ R_2^{*} < a_{i,j}^{*} < G_1^{*}; \\ \left| (a_{i,j}^{*} - R_1^{*}) / (G_2^{*} - R_1^{*}) \right|, if\ b_{i,j} = Y\ and\ G_2^{*} < a_{i,j}^{*} < R_1^{*}; \end{cases}$$

For all current density maps from the *ST-T* interval the consistency of map classes $C_1,\ldots,C_M$ is defined by the following decision rule:

$$C_m = \begin{cases} 0, if\ \lambda \geq \lambda_0; \\ 1, if\ \lambda_1 \leq \lambda < \lambda_0; \\ 2, if\ \lambda_2 \leq \lambda < \lambda_1; \\ 3, if\ \lambda_3 \leq \lambda < \lambda_2; \\ 4, if\ \lambda < \lambda_3. \end{cases}$$

In order to increase the classification reliability the algorithm obtains the following additional features: *specific clusters* are identified as well as the *maximum distance* between them. Map class value will be augmented if there is more than one cluster and a long maximum distance.

Specific cluster consists of *adjacent* vectors with directions corresponding to *G* or *Y* sectors and having length greater than given length l_1. Value of l_1 is determined by formula:

$$l_1 = (\max_{i,j=1}^{10} l_{i,j}) \times p_1,$$

where $l_{i,j}$ is the length of vector located in the i-th column and j-th row of the given map, p_1 is the given threshold which is determined by formula $p_1 = p_0 - 0.2$. So p_1 = 0.6 if p_0 = 0.8. In this case only vectors with length more than 60% of the maximum length (so-called *60% vectors*) may belong to a cluster. Each cluster must contain at least one vector with length more than l_0 (so-called *80% vectors*). Two vectors are considered to be *adjacent* if they are located in the neighboring rows and/or columns. Two selected vectors are grouped into one cluster if they are adjacent (s. Figure 17).

Distance d_{k_1,k_2} between two clusters k_1 and k_2 is calculated by formulas:

$$d_{k_1,k_2} = \min_{\substack{1 \leq i \leq q_1 \\ 1 \leq j \leq q_2}} d(v_i^{k_1}, v_j^{k2}),$$

$$d(v_i^{k_1}, v_j^{k_2}) = \max \{ \left| c_{v_i^{k_1}} - c_{v_j^{k_2}} \right|, \left| r_{v_i^{k_1}} - r_{v_j^{k_2}} \right| \},$$

where: $v_i^{k_1}$ is the *i*-th vector of the k_1-th cluster, $v_j^{k_2}$ is the *j*-th vector of the k_2-th cluster, q_1 – quantity of vectors in the cluster k_1, q_2 – quantity of vectors in the cluster k_2, $d(v_i^{k_1}, v_j^{k_2})$ is the distance between vectors $v_i^{k_1}$, $v_j^{k_2}$, $c_{v_i^{k_1}}$ and $c_{v_j^{k_2}}$ are the indexes of column of the vectors $v_i^{k_1}$ and $v_j^{k_2}$, $r_{v_i^{k_1}}$ and $r_{v_j^{k_2}}$ are the indexes of row of the vectors $v_i^{k_1}$ and $v_j^{k_2}$.

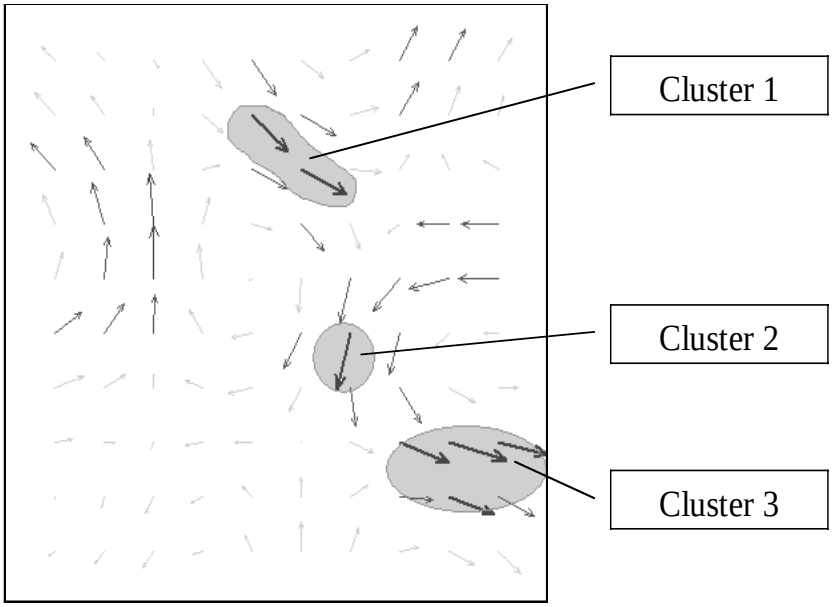

Figure 17: Example of current map with 3 separate clusters

Maximum distance between two furthest clusters is calculated by formula:

$$d = \max_{\substack{1 \le k_1 \le N \\ 1 \le k_2 \le N}} d_{k_1,k_2},$$

where *N* is the number of clusters. If there is only one cluster in the map, *maximum distance* value is considered to be 0. Following map class value correction is performed according to the obtained *maximum distance* value:

$$\begin{cases} C_m^* = C_m, \text{ if } d < 2; \\ C_m^* = C_m + 1, \text{ if } 2 \le d < 4; \\ C_m^* = C_m + 2, \text{ if } d \ge 4. \end{cases}$$

As map the class value can't be more than 4, following correction is performed:

$$\begin{cases} C_m^{**} = C_m^*, \; if \; C_m^* \le 4; \\ C_m^{**} = 4, \; if \; C_m^* > 4. \end{cases}$$

The final step of algorithm is calculation an averaged class C_0 for all maps within ST-T interval by formula

$$\overline{C} = \sum_{i=m}^{M} C_m^{**} .$$

2.4. Assessment of coronary artery disease

Coronary angiography and left heart catheterization were acquired in multiple projections using the Judkins technique according to standard clinical practice (Siemens Cathcor, Erlangen, Germany) in close time relationship (within 24 hours) to the MCG recording.

From the coronary angiograms two experienced observers assessed the degree of stenosis visually in the major branches. Only those patients with narrowing of the coronary arteries ≥ 50% in ≥ 1 vessel were included in this study. No quantitative assessment of individual lesions was made.

2.5.Statistical analysis

Values are given as means ± standard deviation. The portion of each class of map distribution was calculated and compared between the groups on the basis of the Mann-Whitney-U test. The difference in mean level of averaged map class in groups examined also was estimated by Mann-Whitney-U test. A p value of < 0.05 was considered statistically significant.

Averaged map class was used to examine sensitivity and specificity in the prediction of CAD. Sensitivity was defined as the percentage of CAD patients classified by the test to the CAD group and specificity as the percentage of the healthy controls classified to the control group. Cut-off value was defined on the basis of the ROC. Besides probability that , with a positive diagnostic test result, the disease is actually present (PPV), as well as probability that , with a negative test result, the disease is not present (NPV) were calculated.

3. RESULTS

3.1 Reproducibility of maps classification

Over all volunteers included in this group 20.9 ± 1.7 per person were generated in average. The majority of maps was classified as category 0,1 or 2. To quantify the difference between the first recording and second recording (run-to-run reproducibility) and between the first recording and third recording (day-to-day reproducibility) between both groups we compared the percentage of each single class of map distribution on the basis of the Mann-Whitney-U test. The differences were statistically insignificant for all classes both between the first and second measurement(Table II), and between the first and third measurement (Table III).

Table II: Comparison of the percental portion of each class of map distribution; p values are given for the difference between the first and second measurement (run-to-run reproducibility).

Class	*p value*
0	> 0,1
1	> 0,1
2	> 0,1
3	> 0,1
4	> 0,05

Table III: Comparison of the percental portion of each class of map distribution; p values are given for the difference between the first and third measurement (day-to-day reproducibility).

Class	*p value*
0	> 0,1
1	> 0,1
2	> 0,1
3	> 0,1
4	> 0,1

The differences of averaged map class C_0 also was statistically insignificant both between the first and second measurement and between the first and third measurement (Table IV).

Table IV: Average map class C_0 for the first , second and third measurement.

1-st measurement	2-nd measurement	3-rd measurement
1,1±0,5	1,1±0,7	1,2±0,5

Note: $P_{1-2} > 0.1$; $P_{1-3} > 0.1$

Examples of CDV maps within ST-T interval (the first, second and third measurements) are presented on Figure 18 A, B,C.

3.2 Results of maps classification in patients with CAD in comparison with healthy volunteers

In subject 12-lead surface ECG was normal or revealed slight changes in repolarization such as inversion of T-wave no more then in 2 leads. The blood pressure was ≤ 140/90 mmHg in all subjects at the time of MCG registration.

On the basis of coronary angiography, 37 patients had single vessel disease, 37 two and another 34 patients three vessel disease.

Over all subjects 22.1 ± 1.9 maps per person were generated in average.

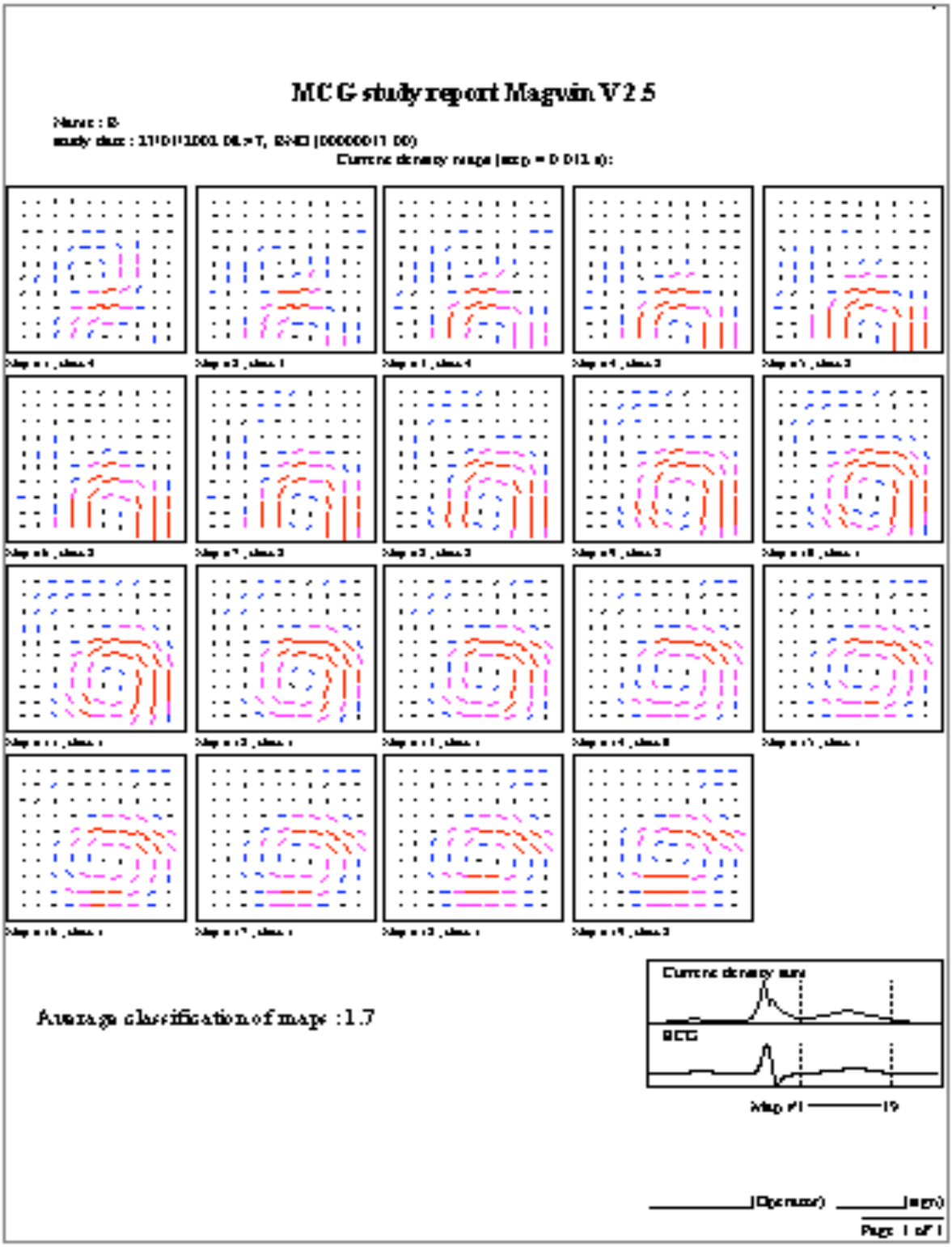

Figure 18 A: Example of CDV maps within ST-T interval of volunteer B.
(the first measurement)

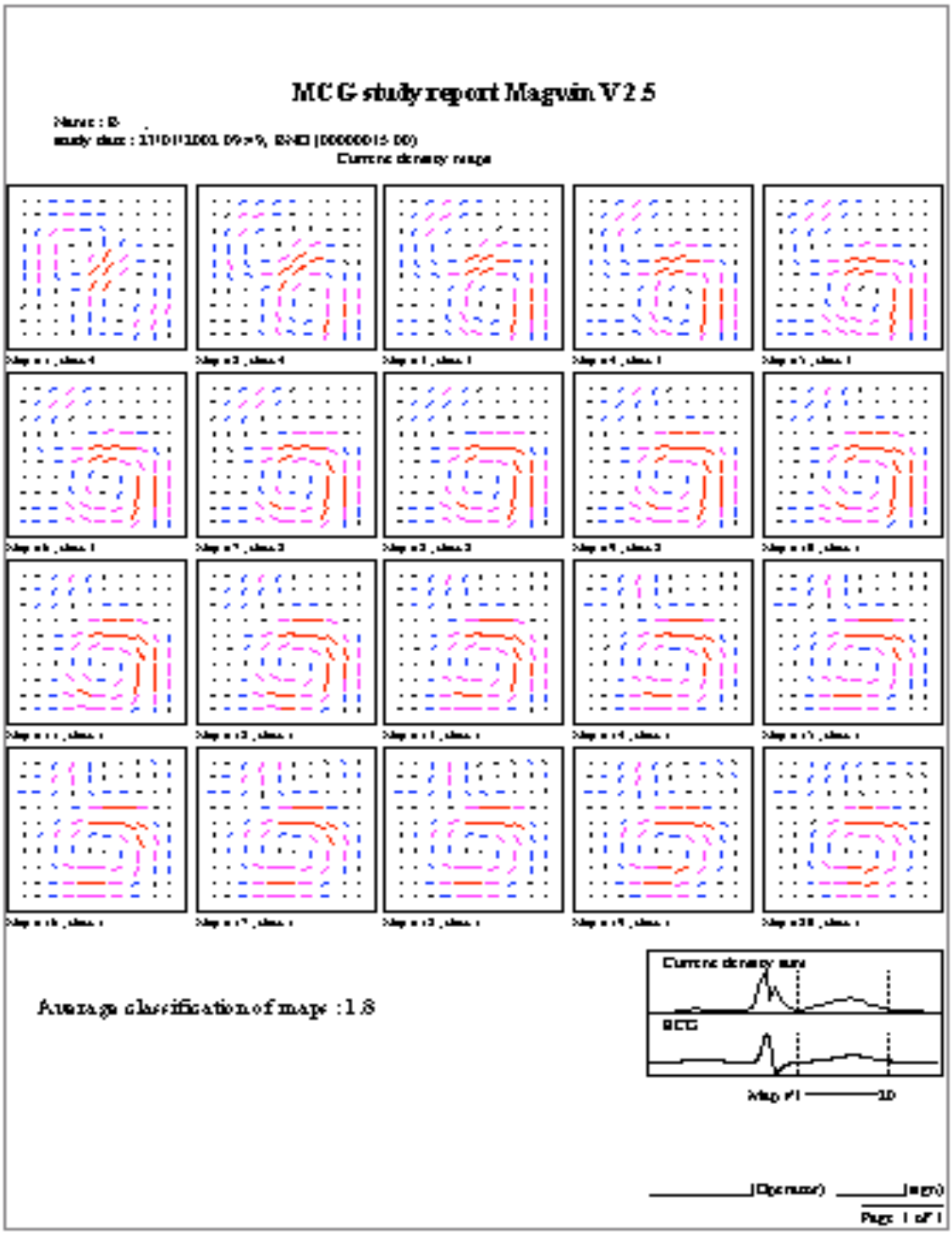

Figure 18 B: Example of CDV maps within ST-T interval of volunteer B.
(the second measurement)

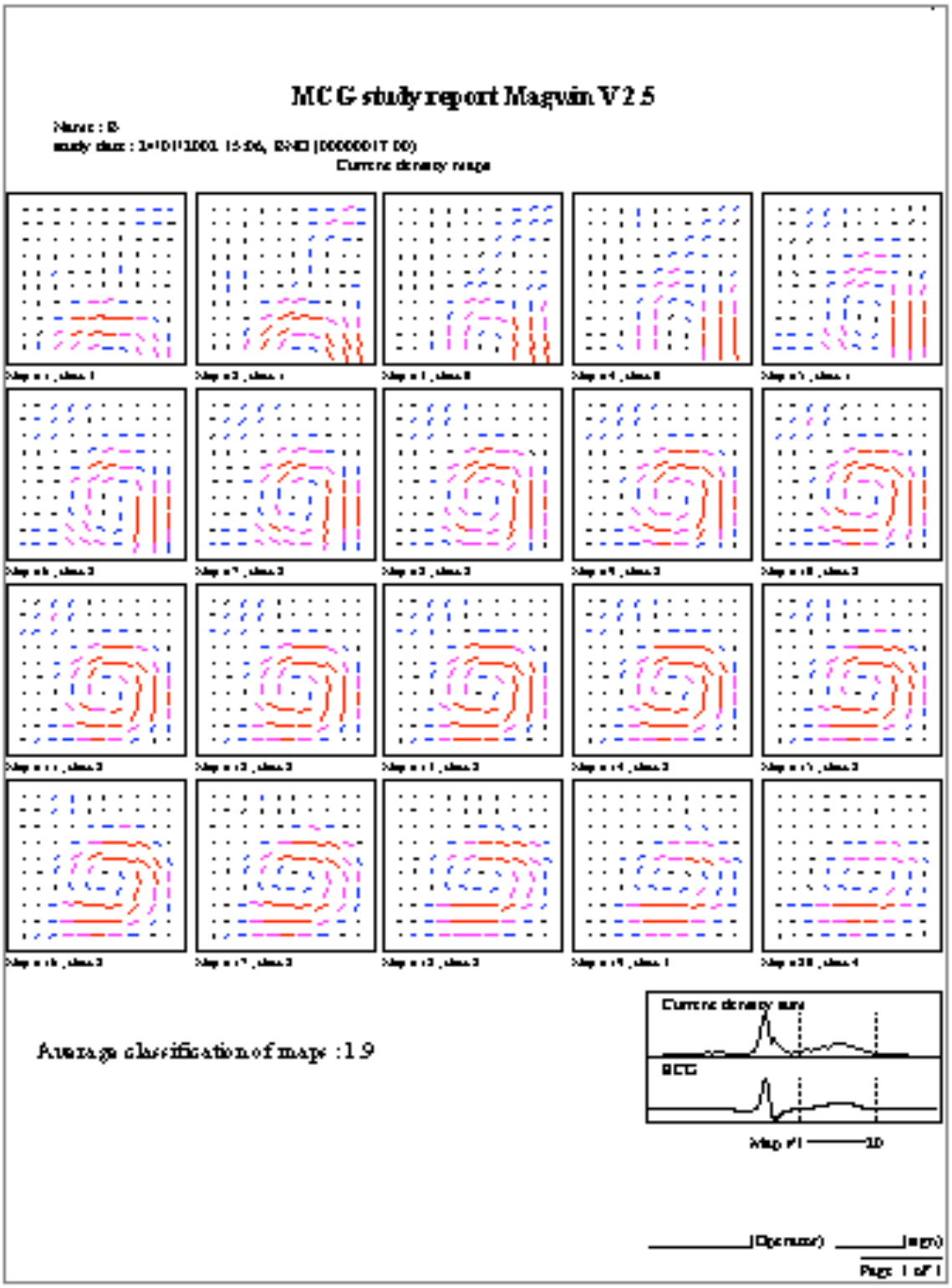

Figure 18 C: Example of CDV maps within ST-T interval of volunteer B.
(the third measurement)

The distribution of the CDV maps categories differed between the subject groups: in normals the majority of maps was classified as category 0, 1 or, rarely, 2 when compared to patients with CAD in whom the categories 3 and 4 were found more often.

The difference in percentage each single class of map distribution between patients with CAD and healthy volunteers were statistically significant for all classes (Table V).

Table V: Comparison of the percental portion of each class of map distribution. p values are given for the difference between CAD patients and healthy volunteers.

Class	*p value for comparison CAD - N*
0	0,001
1	0,001
2	0,002
3	0,01
4	0,001

The difference of C_0 between both groups also was highly statistically significant (Table VI).

Table VI: Average map class C_0 for CAD patients and healthy volunteers.

Groups examined	C_0
Patients with CAD, n = 108	2,42 ± 1,05
Healthy volunteers , n = 97	1,2 ± 0.72

Note: P< 0,0001

Further , analysis of C_0 in accordance to numbers of vessels occluded was done . There is a tendency for increasing of C_0 in patients with the higher number of vessels occluded but differences were statistically insignificant (Table VII).

Table VII: Average map class C_0 in accordance to number of vessels occluded.

Number of vessels occluded	C_0
1 vessel , n = 37	2,.22 ± 0,89
2 vessels , n = 37	2,36 ± 1,15
3 vessels , n = 34	2,7 ± 1,07

Note: $P_{1-2} > 0,1$; $P_{1-3} > 0,1$; $P_{2-3} > 0,1$

Among patients with 1-vessel disease analysis of C_0 in accordance to type of the coronary artery occluded. There were no statistically significant difference between patients with occlusion of LAD, LCX and RCA (Table VIII).

Table VIII: Average map class C_0 in patients with 1-vessel disease in accordance to type of the coronary artery occluded.

Coronary artery occluded	C_0
LAD , n = 17	2,08 ± 0,99
LCX, n = 13	2,43 ± 0,85
RCA, n = 7	2,2 ± 0,73

Note: $P_{1-2} > 0,1$; $P_{1-3} > 0,1$; $P_{2-3} > 0,1$

To diagnose CAD based on C_0 value the following binary decision rule was proposed:

$$\textit{Person is CAD, if } \overline{C} > C_0,$$

$$\textit{Person is Healthy, if } \overline{C} < C_0.$$

To define the diagnostic usefulness of this rule and to determine the optimal value of the threshold C_0 we used ROC analysis[14] and constructed the receive operation characteristic which shows the relationship between sensitivity S_E and specificity S_P of this test under different values of C_0 threshold. The plot of the ROC curve is shown on Figure 19.

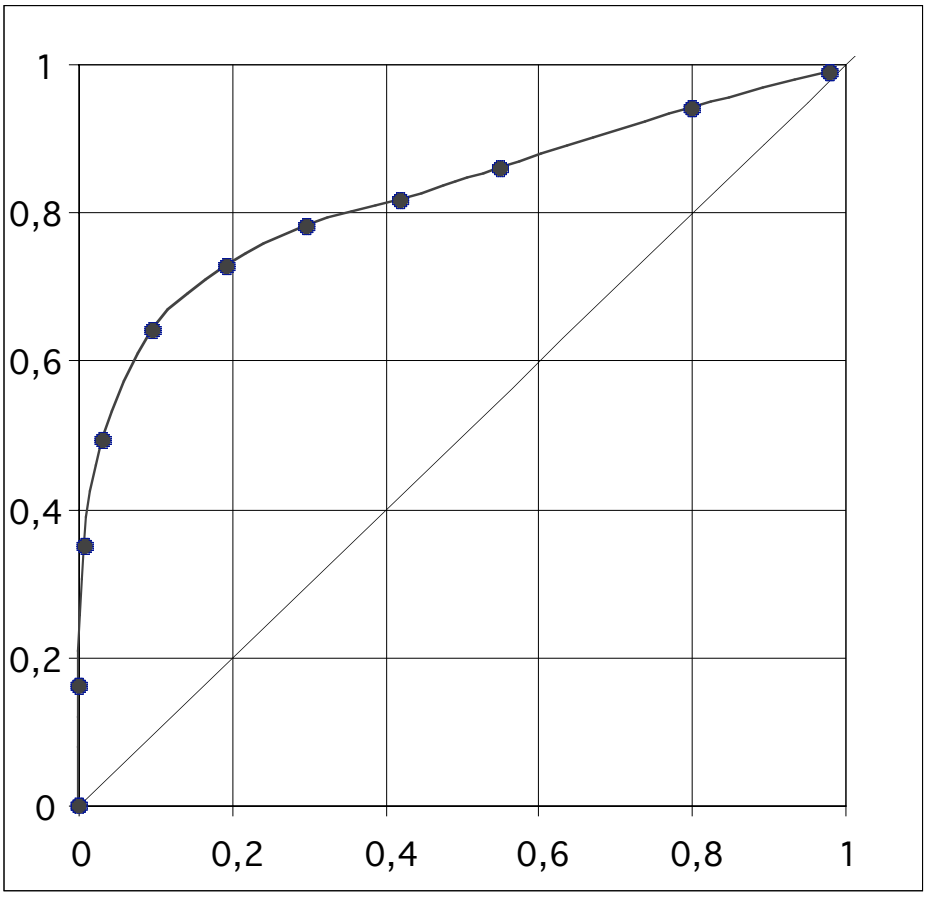

Figure 19: Receive operation curve for groups examined

The threshold value with the maximal discriminative power is equal C_0 =1,75. Subjects with the averaged map class higher than 1,75 were classified as CAD patients, subjects with a map class lover than 1.75 were classified as normal. With this threshold 80 of 108 patients with CAD and 78 of 97 healthy volunteers were classified correctly (Table 9).

Table IX: Sensitivity , Specificity , PPV, NPV of CAD detection with the threshold C_0 =1,75

Sensitivity	**74%**
Specificity	**80%**
PPV	**81%**
NPV	**73,5%**

Typical examples of CDV maps within ST-T interval of patient with CAD and healthy volunteers are presented on Figure 20 A, B.

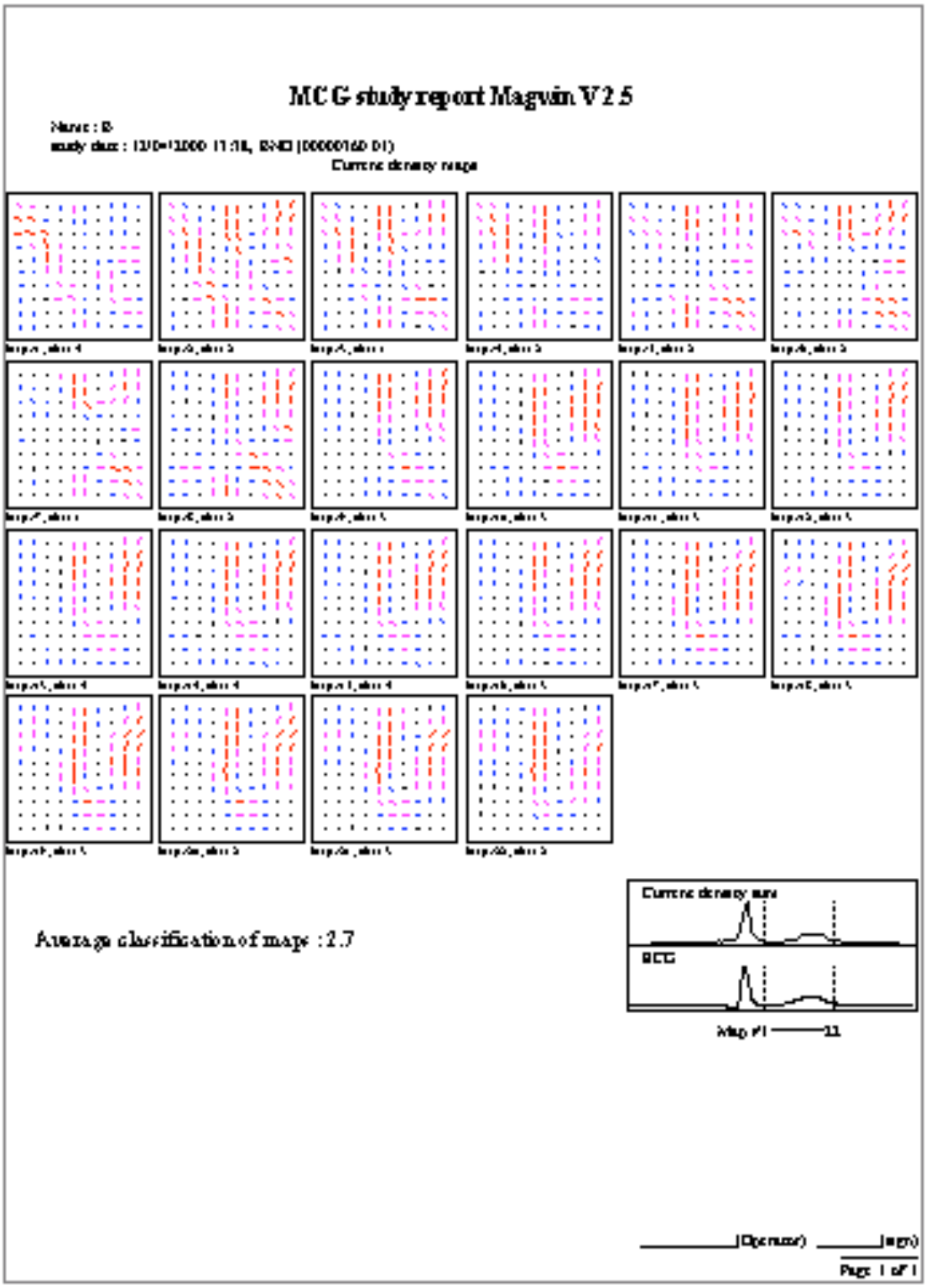

Figure 20 A: Example of CDV maps within ST-T interval of patient B. with 2-vessels disease

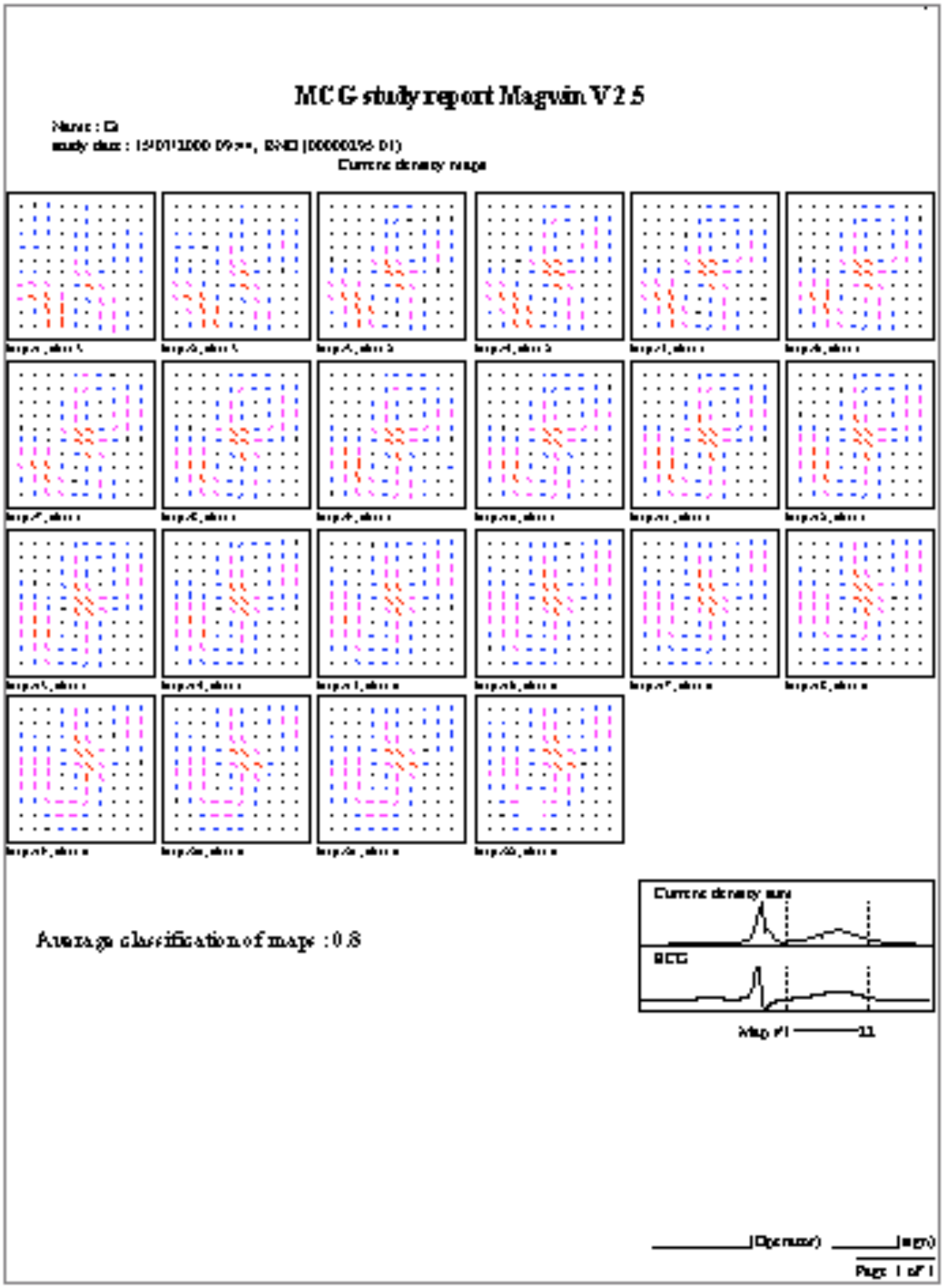

Figure 20 B: Example of CDV maps within ST-T interval of healthy volunteer B.

4. DISCUSSION

4.1. Main findings

Magnetocardiographic mapping at rest can detect myocardial ischemia in a heterogeneous CAD population including subsets of patients with ischemia in any of the main coronary artery branches regions but without prior myocardial infarction and with normal 12-leads ECG at rest .

Simple magnetocardiographic system, installed in unshielded location is capable to be a reliable diagnostic instrument.

4.2. Clinical implications

In assessing patients with confirmed or suspected cardiac disease , noninvasive strategies are on increasing clinical importance to avoid serious side effect and expanding costs that are often associated with invasive methods. The focus is the management of patients with chest pain.

Coronary angiography remains the gold standard for the identification of hemodynamically significant CAD but should be restricted to symptomatic patients because of its invasive character, risk and cost.

The noninvasive diagnosis of cardiac ischemia related to CAD remains a clinical challenge The 12 lead electrocardiogram at rest is frequently normal in such patients and the predictive value of other methods like exercise-ECG (SIMOONS and HUGENHOLTZ, 1977), stress echocardiography (COHEN at al., 1995) or nuclear imaging (ZARET at al.,1993; ZIMMERMANN at al., 2002) is often limited. Its performance may be associated with a certain risk .Recent developments include new imaging techniques like scintigrapphy, positron emitting tomography, electron-beam computed tomography, magnetic resonance imaging or spiral computed tomography (PRASAD at al., 2004).

Despite good values for sensitivity, specificity remains unsatisfactory in some studies (SCHMERMUND at al.,1999). Besides these methods require external or internal radiation , and , therefore, can not be conducted in some patients (for example, in the case of pregnancy). Other limitations are contraindications to the administration of intravenous iodinated contrast material (for example , allergy, renal failure, or hyperthyroidosms).

The value of the 12 lead ECG can be augmented by the measurement of electrical activity at more registration sites. On the basis of BSPM anomalous repolarization patterns have been demonstrated in patients with ischemic heart disease at rest not apparent in the 12-lead ECG (STILLI at al.,1986; MONTAGUE at al.,1990; KITTNAR at al.,1993). However this method itself is also limited because of the time consuming procedure of lead placement and registration. Analogous to BSPM, MCG can register cardiac activity at multiple sites over the heart , while the signal can be processed and analysed in a fashion similar to the computerized ECG . In addition the increase in the number of registration sites from the MCG augments the information on the cardiac de- and repolarization process. Furthermore the method itself is completely noninvasive in that even skin contact is unnecessary. However, the acceptance of MCG in clinical practice remained limited mainly because of the high costs required for the installation of the system inside a magnetically shielded setting. With the recent development of a totally new, highly sensitive, device not requiring any shielding, a new option was created to determine whether measurement of the magnetic field of the heart was superior to the assessment of the surface potentials on the chestcage which currently remain the routine.

The present study analyzed only cardiac repolarization in healthy subjects and in patients with CAD without MI under resting conditions with a four-channel MCG system outside a shielded room. As in none of the patients and controls the 12 lead ECG revealed typical changes in repolarization suggesting the diagnosis of myocardial ischemia, it is

striking that the MCG showed obvious differences between both groups on the basis of maps reconstructing the current density distribution . Healthy subjects displayed the area of main current density vectors in the center or left part of most maps during the ST-T interval directed left downward within a 10° to 80° sector. Most maps within the ST-T interval were classified as class 0, 1 or 2. In CAD patients we could see two obvious differences: First of all there was a change in the direction of the main current vector with a deviation more to the right or left upward. The second difference refers to the non dipolar structure of these maps. The percentage of each class of map within the ST-T interval was statistically significant between CAD patients and healthy subjects for each class. All controls fell in class 0,1 or 2 (normal current distribution) while all patients demonstrated mainly maps of class 3 or 4 (pathologic current distribution).

These differences between healthy subjects and CAD patients at rest could be explained from a pathophysiological point of view by the assumption of a more inhomogeneous repolarization process in CAD patients, an explanation that would presume the presence of myocardial ischemia at rest. Indeed the very absence of ischemia under resting conditions is generally accepted to be the explanation for a normal ECG at rest in CAD patients. Keeping in mind that ischemia is a dynamic process with an important temporal continuum starting with changes on molecular basis followed by some unspecific changes in the 12 lead standard ECG progressing , leading to wall motion disturbances, and angina as a last step, it could be possible that this new method is able to detect signs of ischemia in a very early phase of such a dynamic process(YAN at al.,1993)

The causes of electrical inhomogeneity are manifold. There is first of all the change of repolarization as a result of apoptosis (BUJA and ENTMANN , 1998). Also earlier episodes of myocardial ischemia could have led to circumscribed regions of cell necrosis resulting in impaired electrogenesis. Finally there are a multiple of shifts in ionic transfer.

In the current discussion concerning the advantages of MCG over ECG it has been pointed out that MCG is more sensitive not only to tangential but also to vortex currents in the heart than the ECG (KOCH, 2001).

The method like BSPM which analyzes cardiac repolarization in more detail than the ECG also could identify CAD in patients with a normal ECG at rest. This superiority of BSPM over 12-lead ECG might be the result of the registration technique itself as cardiac activity is measured at multiple points above the thorax thus increasing the information about cardiac electrogenesis (MIRVIS , 1985; SASAKI at al., 1997).

MCG is expressed im µAmpere only similar to BSPM measured in minivolts to the extent that the number of registration sites is increased in the latter when standard (LANT at al., 1990) . Using this potential for the analysis of spatial aspects of cardiac activity it was shown previously by HAILER (1999) that CAD patients could be identified at rest because of their increased heterogeneity of repolarization as revealed by temporal and spatial changes of QT dispersion. The current density vector map reconstruction is another approach to visualize the cardiac repolarization process.

The results of earlier studies with multichannel MCG systems inside a shielded setting were always limited by the expensive costs of the system itself and by the lack of simple diagnostic procedures (MOSHAGE at al., 1991; SATO at al., 2000; , HANNINEN at al., 2001). A fast, reproducible and practical concept of data analysis is an obligatory requirement for the wide clinical acceptance of the method. The computer system for CDV maps classification, which is used in this study, is based on well-understandable parameters of current distribution in the course of ventricular repolarisation: homogeneity of the process and direction of the vectors.

This system allows to assign automatically one single measurement as normal or pathological based on an average map class value. The parameters tested had low

disagreement between repeated measurements, as the operation of the system is computer-controlled and it provides parametric values.

There is a tendency to increase the average map class inhomogeneity level in patients with the higher number of vessels occluded, but this tendency is not statistically significant. This might be explained by the fact that degree of myocardial ischemia and , hence, degree of electrical inhomogeneity do not depend only on number of vessels occluded , but also caused by level of occlusion and status of collateral circulation. These parameters were not controlled in the study.

In the case of 1-vessel disease there is not statistically significant difference of average map class in accordance to type of coronary artery occluded.

Although there seemed to be a relationship between the deviation of the main current vectors and the affected coronary vessel, this dependency given the small series of observations was not strong enough to predict the localization of myocardial ischemia on the basis of the MCG result.

However, the fact that CAD patients, presumably with ischemia but normal ECG at rest, might be identified on the basis of a completely noninvasive method with the help of relatively simple system is of clinical interest.

The present data show the results of a inexpensive four-channel system not requiring a shielded room. Magnetocardiography in unshielded location , with a low per-test cost , might provide the potential reduction in hospital expenditures by improved identification of cardiac ischemia and more effective exclusion of non-ischemic patients from further testing. A further confirmation of the results , presented in these study, in a greater population would be an important step towards the aim to restrict invasive procedures like coronary angiography to those patients in whom the diagnosis of CAD is

confirmed prior to the procedure and in whom interventional therapy appears to be indicated.

4.3. Methodological considerations

Several aspects may be considered.

The 4-channel system with 4.5-5 minutes of examination procedure duration allows no temporal synchrony between the registration sites. If there is a substantial change in heart rate during acquisition this may lead to distortions in the CDV maps. This disadvantage can be abolished by ongoing developments of software and more multichannel systems. On the other hand the absolute temporal conformity seems to be of no great importance for the analysis of more stable processes like cardiac repolarization under resting condition. In our experience heart rate changes are minimal and need not to be taken into consideration. This would be completely different for the examination of cardiac arrhythmias and also for examinations under stress.

The presence of residual noise resulting from unshielded setting might have influenced the results. This influence should be controlled more objectively , based on special software.

Quantitative analysis of the coronary arteriogram should be done. This analysis will allow to investigate in more details the relationship between MCG results and the location of the coronary artery lesions , degree of stenosis , as well as the degree of perfusion and filling expressed as TIMI flow.

All CAD patients were on appropriate anti-anginal medication. For safety reasons these medications were continued during the study.

Further research has to be done in order the influence of medication such as ß-blocker antagonists or ACE inhibitors on the CDV maps.

4.4. Prospects of further improvements of MCG data analysis

To establish MCG in clinical practice, the presentation of MCG data should be improved. Cardiologists are unfamiliar with the images currently produced by MCG. It is therefore of utmost importance to present the information currently presented in a digital formula in “absolute terms“ like for all other comparative methods. “Absolute terms“ for MCG, primarily analyzing homogeneity of electrical properties of the myocardium may be the dispersion of conduction velocity within certain physiological periods of the cardiac cycle, mainly during ventricular repolarization.

It is expected that adequate software allowing differentiating between areas of hypo-, hyper- or normal conduction as well as diagnostic indicators is available. This will allow to image the heart magnetocardiographically in a way cardiologists are used to see e.g. perfusion defects in scintigraphic or PET images.

5. SUMMARY

The aim of this was to examine the capability of magnetocardiographic mapping at rest using a simple system, installed in unshielded location, to detect myocardial ischemia in a heterogeneous CAD population including subsets of patients with ischemia in any of the main coronary artery branches regions but without prior myocardial infarction and with normal 12-leads ECG at rest .

A total of 110 patients with CAD and 98 healthy controls were included in the study. Another 15 volunteers with no history of any cardiovascular disease were used for run-to-run and day-to-day reproducibility assessment .

MCG recordings were taken with the help of four-channel SQUID-magnetometer system , installed in unshielded setting, at 36 pre-thoracic sites over the pericardial area. For further analysis the reconstruction of CDV maps within the ST-T interval was applied. Each CDV map was classified automatically by means of a classification system with a scale from 0 to 4 with increasing abnormality . The averaged class was calculated for each subject in order to discriminate between groups.

The results showed that CDV maps of healthy volunteers have mainly dipolar structure with only one area of larger vectors directed left – downwards. In contrast the CDV maps of patients with CAD demonstrate mainly non-dipolar structure with additional areas of larger current vectors.

With the threshold 1,75 of average map class sensitivity 74% , specificity 80% , PPV 81 % , NPV 73,5 % were achieved .

The parameters tested had low disagreement between repeated measurements. Relatively simple 4-channals system , installed in unshielded location, was robust in operation, signal quality was good enough for the analysis.

Results were discussed.

6. REFERENCES

1. Achenbach, S., Moshage, W., Fürst, S.(1995).: Investigation of magnetocardiographic parameters for the detection of graft rejection after heart transplantation.
In: Baumgartner C., Deecke L., Stroink G., Williamson S.J.(Eds.): Biomagnetism: Fundamental research and clinical applications. P.619-623.
Amsterdam, IOS Press

2. Adams A, Stroink J, Van Leeuwen P , Hailer B.(1998) :
KLT Analysis of QRST integral maps of patients with and without CAD at rest and during pharmacological stress.
In: Yoshimoto T., (Ed.) : Recent advances in biomagnetism . P.998-1001.
Sendai: Tohoky University Press

3. Agraval R., Czerski K., Goedde , P. Kuehl , U. (2000) : Noninvasive follow up of evolution of myocarditis .
In: Nenonen J., Katila T.(Eds.): Proceedings of the 13-th International Conference on Biomagnetism . P. 527-529.
Helsinki: University of Technology

4. Baule, G., McFee, R .(1963):
Detection of the magnetic field of the heart.
Am. Heart J.66.95-96.

5. Bobrov V., Chaikovsky I., Stadnyk L., (1997)
Study of diagnostic value of integrated MCG.
Biomedizinische Technik. 42 (Suppl.1). 142-144.

6. Bobrov V.,Gapeluk A., Chaikovsky I., Stadnyuk L., Sosnitsky, V., Kozlovski V (2000).
Contraventions of homogeneity of ventricular repolarisation according to data of Magnetocardiography and their Connection with Ventricular Tachycardia.
In: Aine C., Stroink G., Wood C., Okada Y., Swithenby S. (Eds.): Proceedings of the 10-th International Conference on Biomagnetism. P. 440-443.
New York : Springer-Verlag Inc.

7. Brockmeier K., Schmitz L., Bobadilla-Chavez J.D., Burghoff M., Koch H., Zimmermann R., Trahms L (1997) :
Magnetocardiography and 32-lead potential mapping: repolarization in normal subjects during pharmacologically induced stress.
J. Cardiovasc.Electrophysiol. 8. 615-626.

8. Buja LM., Entman ML.(1998):
Models of myocardial cell injury and cell death in ischemic heart disease.
Circulation 98. 1355-1357.

9. Chaikovsky I.,Stadnyk L., Sledzevskya I., Bilinsky E., Sosnytsky V. ,Steinberg F, Budnik N. (1999) : Changes in Magnetic field maps in patients with acute non-Q myocardial infarction.
In: Universitat Witten/Herdecke , Scientific issue, P.12-17.
Essen

10. Chaikovsky I., Lutai M., Lomakovsky A., Gapeluk A., Sosnitsky V., Minov Yu.(2000) : Ventricular repolarisation disturbances diagnostics in chronic ischemia patients evidence derived from MCG.
In: Aine C., Stroink G., Wood C., Okada Y., Swithenby S. (Eds.): Biomag96:Proceedings of the 10-th International Conference on Biomagnetism. P. 444-447.
New York : Springer-Verlag Inc.

11. Chaikovsky I. , Kohler J., Hecker Th. , Hailer B. , Auth-Eisernitz S. , Sosnytsky V., Feinzilberg L. , Budnik N. , Steinberg F. (2000) : Detection of coronary artery disease in patients with normal or unspecifically changed ECG on the basis of magnetocardiography.
In: Nenonen J., Katila T.(Eds.): Proceedings of the 12-th International Conference on Biomagnetism . P. 565-568.
Helsinki: University of Technology Press

12. Chaikovsky I. , Primin M ., Nedayvoda I. , Vassylyev V , Sosnitsky V., Steinberg F.(2002): Computerized classification of patients with coronary artery disease but normal or unspecifically changed ECG and healthy volunteers. ´
In: Nowak H., Haueisen J., Giessler F., Huonker R. (Eds.) :Biomag 2002: Proceedings of the 13-th International Conference on Biomagnetism . P. 534-536
Berlin :VDE Verlag

13. Chaikovsky I., Katz D., Katz M.(2003):
Principles of magnetocardiographic maps classification and CAD detection.
International Journal of Bioelectromagnetism 5. 100-101.

14. Cohen, D., Edelsack , E.A. , Zimmerman , J.E. (1970):
Magnetocardiograms taken inside a shielded room with a superconducting point-contact magnetometr.
Appl. Phys. Lett. 16.278-280.

15. Cohen JL, Chan KL, Jaarsma W, Bach D, Muller D, Starling M, Armstrong W. (1995):
Arbutamine echocardiography: efficacy and safety of a new pharmacologic stress agent to induce myocardial ischemia and detect coronary artery disease.
J Am. Coll. Cardio. 26. 1168-1175.

16. Cremer P. , Leeuwen P. Van, Hailer B., Lange S., Grönemeyer D. (1999):
Changes in magnetic field during repolarization in patients with coronary artery disease.
Med. & Biol. Eng. & Comput. 37 (Suppl.2) . 1480-1481.

17. Gapeluk A., Schirdewan A , Shuett H., Selbig D., Zimmermann R., Primin M. (1998) :
Magnetocardiographic diagnostics of patients with ischemic heart disease.
In: 11-th International Conference on Biomagnetism , Book of abstract. P. 119.
Sendai

18. Gödde P., Müller H.-P., Czerski K., Endt P., Steinhoff U., Oeff M., Schultheiss H.-P.(2001) :
Magnetocardiographic mapping of QRS Fragmentation in patients with a history of malignant tachyarrhythmias.
Clin. Cardiol. 24. 682-688

19. Hailer B. , Van Leeuwen P. , Lange S. , Grönemeyer D. , Wehr M.(1998) :
Spatial Dispersion of the Magnetocardiographically determined QT Interval and its components in the identification of patients at risk for Arrhythmia after Myocardial Infarction.
A.N.E 3. 311-318

20. Hailer B. , Van Leeuwen P. , Lange S., Pilath M., Wehr M.(1999) :
Coronary Artery Disease May Alter the Spatial Dispersion of the QT Interval at Rest.
A.N.E. 4. 267-273

21. Hailer B., Chaikovsky I., Auth-Eisernitz S., Shäfer H., Steinberg F., Grönenemeyer D.H.W.(2003):
Magnetocardiography in coronary artery disease with a new system in an unshielded setting.
Clin.Cardiol. 26. 465-471

22. Hailer B., Chaikovsky I., Auth-Eisernitz S., Shäfer H., Van Leeuwen P.(2005):
The value of magnetocardiography in patients with and without relevant stenoses of the coronary arteries using an unshielded system.
PACE 28 . 8-15.

23. Hanninen H., Takala P., Makijarvi M. (2000):
Detection of exercise-induced myocardial ischemia by multichannel magnetocardiography in single vessel coronary artery disease.
A.N.E. 5. 147-157.

24. Hamalainen M.S., Nenonen J.(1999): Magnetic source imaging .
In: Webster J.(Ed.): Encyclopedia of Electrical Engeneering. Vol.12. P.133-148.
New York: Wiley

25. Katayama M., Nomara M., Nakaya Y. (1989) :
QRS wave of the magnetocardiogram in right ventricular overload: correlation with right ventricular messare.
Am. J. Noninvas. Cardiol. 3. 110-115.

26. Katayama M., Nakaya Y.(1990):
The magnetocardiographic diagnosis of right ventricular diastolic overload.
Fokushima I. exp. Med. 37. 9-21.

27. Katz D., Naber C., Katz M., Chaikovski I., Wieneke H., Erbel R. (2003):
Magnetocardiography as a sensitive method for detecting a coronary stenosis of the left descending artery.
JACC. 41 (Suppl A). 436A.

28. Kittnar O., Slavicek ., Vavrova M.(1993):
Repolarization pattern of body surface potential maps (BSPM) in coronary artery disease.
Physiol. Res. 42. 123 .

29. Koch, H.(2001):
SQUID MCG: Status and Perspectives.
IEEE Trans. Appl. Supercond. 11. 49-59.

30. Lant J, Stroink G, ten Voorde B, Horacek BM, Montague J(1990):
Complementary nature of electrocardiographic and magnetocardiographic data in patients with ischemic heart disease.
J. Electrocardiol. 23. 315-322.

31. Lant J., Stroink G., Montague TJ.(1991)
Discrimination between infarct groups through the use of iso-integral magnetic field maps.
A.N.E. 5, 215-222.

32. Leder U., Pohl H.-P., Michaelsen S., Fritschi T., Huck M., Eichhorn J., Muller S., Nowak H.(1998) :
Noninvasive biomagnetic imaging in coronary artery disease based on individual current density maps of the heart.
Int.J. Cardiol. 64. 83-92

33. Makela T., Pham QC., Clarysse P., Nenonen J., Lotjionen J., Sipila O., Hanninen H., Lauerma K., Knuuti J., Katila T., Magnin IE.(2003):
A 3-D model-based registration approach for the PET, MR and MCG cardiac data fusion.
Med. Image Anal. 7 (Suppl. 3). 377-389.

34. Mirvis DM.(1985):
Spatial variation of QT intervals in normal persons and patients with acute myocardial infarction.
JACC 3. 625-631.

35. Morguet AJ., Koch H., Kosch T., Behrens S., Lange C., Wunderlich W., Selbig D., Munz DL., Schultheiss HP.(2002):
Differentiation between vital heart muscle tissue and infarct scar using magnetocardiography.
Biomedizinische Technik. 47 (Suppl.1). 538-540.

36. Montague TJ., Witkowski FX., Miller RM., Johnstone DE ., MacKenzie RB., Spencer CA ., Horacek BM.(1990):
Exercise body surface potential mapping in single and multiple coronary artery disease.
Chest 97. 1333-1342.

37. Moshage W., Achenbach S., Weikl A., Göhl K., Bachmann K.(1991):
Clinical magnetocardiography: Experience with a biomagnetic multichannel system.
Int. J. Cardiac Imaging 7. 217-223.

38. Moshage W., Achenbach S., Gohl K., Bachmann K.(1996):
Evaluation of the noninvasive localization accuracy of cardiac arrhythmias attainable by multichannel magnetocardiography(MCG).
Int.J.Card. Imaging. 12. 47-59.

40. Murakami M., Watanabe K., Takeushi A. (1987): The QRS wave of the magnetocardiogram in myocardial infarction.
In : Proc. of 6-th International conference on Biomagnetism, P.354-357.
Tokyo: Tokyo Denki University Press

41. Nomura M., Nakaya Y., Ishihara S. (1989):
Magnetocardiographic studies of ventricular repolarization in old inferior myocardial infarction.
Europ. Heart J. 10, 8-15.

42. Oja O.S., Nousiainen J., Malmivuo J. (1995) : Comparison of the diagnostic performance of magnetocardiography and electrocardiography in anteroseptal and inferior infarction.
In: Baumgartner C., Deecke L., Stroink G., Williamson S.J. (Eds.): Biomagnetism: Fundamental research and clinical applications. P.595-598.
Amsterdam, IOS Press

43. Park JW., Hill PM., Chung N., Hugenholtz PG., Jung F.(2005):
Magnetocardiography predicts coronary artery disease in patients with acute chest pain.
A.N.E. 10. 312-23.

44. Pesola K. , Hanninen H. , Laurema K.(1999) :
Current density estimation of the left ventricular epicardium: A potential method for ischemia localization.
Biomedizinische Technik. 42 (Suppl.1). 143-146.

45. Prasad SK., Assomull RG., Pennel DJ.(2004):
Resent developments in non-invasive cardiology.
BMJ. 329. 1386-1389.

46. Primin M., Chaikovsky I., Berndt C., Nedayvoda I., Korfer J.(2003):
Layer-to-layer heart electrical image based on magnetocardiography data in comparison with perfusion image based on PET.
International Journal of Bioelectromagnetism 5. 27-28.

47. Romanovych S. (1997):
Reconstruction of three components dipoles within layer.
Biomed .Tech. 42 (Suppl 1.). 227-230.

48. Saarinen, M., Siltanen, P.J., Katila T.(1978) :
The normal magnetocardiogram, I. Morphology .
Ann. Clin. Res. 10 (Suppl. 21). 1-43.

49. Schmermund A., Baumgart D., Erbel R. (1999):
Potential and pitfalls of electron-beam computed tomography in detecting coronary atherosclerosis.
Bas Res Cardiol. 94. 427-444.

50. Schmitz L., Koch H., Brockmeier K., Muller J. , Schuler S., Warnecke H., Hetzer R., Erne,S.(1992) : Magnetocardiographic diagnosis of graft rejection after heart transplantation.
In: Hoke M. (Ed.):Biomagnetism : Clinical aspects. P.555-558.
Amsterdam: Elsevier Science Publisher

51. Simoons ML, Hugenholtz PG (1977):
Estimation of the probability of exercise induced ischemia by quantitative ECG analysis.
Circulation 56 . 552-559.

52. Steinberg B., Roguin A., Watkins S., Hill P., Dharsh F., Resar JR.(2005) Magnetocardiogram recording in nonshielded environment- reproducibility and ischemia detection.
A.N.E. 10. 152-160

53. Stilli D., Musso E., Macchi E., Manca. C, Dei Cas. L, Vasini P., Taccardi B. (1986): Body surface potential mapping in ischemic patients with normal resting ECG.
Can J Cardiol. 8. 107A-112A.

54. Stroink G., Lant J., Elliott P., Charlebois P., Gardner M.J.(1999): Discrimination Between Myocardial Infarct and Ventricular Tachycardia Patients Using Magnetocardiographic Trajectory Plots and Isointegral Maps.
J. Electrocardiol. 25. 129-142.

55. Tripp J. H. (1983): Physical Concepts and mathematical models.
In: Williamson S.J., Romani G.-L., Kaufman L., Modena I. (Eds.):Biomagnetism- an interdisciplinary approach.
NATO Advanced Science Institutes Series. Vol. 66 ; P.101 –140. New York , London: Plenum Press

56. Sasaki R, Sugisawa K, Iwasaki T(1997): Use of the body surface recovery time for detection of coronary artery disease.
Jpn .Heart J. 38. 345-360.

57. Sato M., Terada Y., Mitsui T., Miyashita T., Kandori A., Tsukada K.(2001):Detection of myocardial ischemia by magnetocardiogramm using 64-channal SQUID system.
In: Nenonen J., Katila T.(Eds.): Proceedings of the 12-th International Conference on Biomagnetism . P. 523-526.
Helsinki: University of Technology

58. Van Leeuwen P, Hailer B, Wehr M (1997) :
Changes in current dipole parameters in patients with coronary artery disease with and without myocardial infarction.
Biomedizinische Technik. 42. 132-135.

59. Yan GX., Yamada KA., Kleber AG., McHowat J., Corr PB.(1993):
Dissociation between cellular K+ loss, reduction in repolarization time, and tissue ATP levels during myocardial hypoxia and ischemia.
Circ. Res. 72. 560-570

60. Zaret BL, Wackers FJ.(1993):
Medical progress: Nuclear cardiology (second of two part).
N. Engl. J. Med. 329. 855-863.

61. Zimmermann R, vom Dahl J, Schäfers M, Schwaiger M.(2002):
Positionsbericht nuklearkardiologischer Diagnostik – Update.
Z.Kardiol. 91. 88-92.

7. ABBREVIATIONS

BSPM	body surface potential mapping
C_0	average map class
CAD	coronary artery disease
CDV	current density vector
ECG	electrocardiography , electrocardiogram
LAD	left anterior descending coronary artery
LCX	left circumflex coronary artery
MCG	magnetocardiography , magnetocardiogram
MI	myocardial infarction
NPV	negative predictive value
PPV	positive predictive value
RCA	right coronary artery
SD	standard deviation
SQUID	superconducting quantum interference device

8. ACKNOWLEGEMENTS

I would like to express my warmest gratitude to my “Doktorvater” Prof. Prof.h.c. Dr. med. Manfred Blank for his newer-ending support , patience and understanding.

I am very much indebted to Priv.-Doz. Dr.med Birgit Hailer , Head of Medical Clinic II , Phillippusstift , Essen , a distinguished expert in the field of clinical magnetocardiography, for her excellent collaboration and advises throughout many years , for her support of this work and for her kind help in my personal problems.

I am especially thankful to my Ukrainian colleagues and friends from the Institute for Cybernetics of National academy of sciences – Prof. I.Voitovich, Drs. Volodimir Sosnytsky , Yuri Minov , Pavlo Sutkovy, Mukola Budnik , developers of the hardware , for their outstanding enthusiasm and competence .

I am also very much appreciated to excellent mathematicians from the Ukranian academy of sciences: Prof. Leonid Fainzilberg - for the developing of mathematical algorithms of maps evaluation and design of software package MAGWIN; Prof.Yuri Vasetsky – for productive collaboration in the developing of models of currents distribution; Prof. Stanislav Romanovitch - for method of inverse solution.

I express my warmest gratitude to Dr. Peter van Leeuwen , Head of Department of Biomagnetism , EFMT , Bochum , a leading scientist in the area of biomagnetism , who taught me how to do scientific work.

I am sincerely grateful to Prof. Dr.med. Raimund Erbel, Director of Clinic for Cardiology, in Essen University Hospital for his positive view on the method and especially for his extremely valuable advises concerning approaches to maps classification.

I extend my warmest thanks to Prof. Michael Primin , Drs. Valery Vasiliev and Igor Nedayvoda from the Ukranian academy of sciences for teaching me facts about physics

and many innovative scientific discussions during all these years and also for their friendship and moral support.

I extend my warmest gratitude to Dr. med. Sabine Auth-Eisernitz and Eugenia Konjaeva for their contribution in patient measurements , competence and enthusiasm.

I would like to express my warmest thanks to Prof. Paul Hugenholtz , former Head of the Thoraxcentrum of Erasmus University in Rotterdam , for supporting me in my endeavors throughout the years. His advises and friendship were extremely important for me.

I am sincerely grateful to Dipl. Phys. Bernhard Awolin for his excellent contribution in the organization of this work , optimism and support.

I am appreciate to Dr. med. Fritz Steinberg for his grate efforts.

I express my warmest gratitude to the numerous coronary artery disease patients and healthy volunteers who participated in the study. I am deeply indebted to all these people.

My parents , Mariam and Anatoly , deserve my warmest gratitude for their continuous love and support throughout all my life.

9. CURRICULUM VITAE

Personal data:

Name :	Illya Chaikovsky
Date of birth :	27.07.1965
Place of birth:	Kiew , Ukraine
Father:	Anatoly , electrical engineer
Mother:	Mariam , pediatrician
Domicile at the moment:	Essen , Germany

Education:

1995-1998	Post-graduate course of medical cybernetics, Institute for cybernetics of National academy of science, Kiew , Ukraine
June 1989	State Exams on medicine
1983-1989	Tver State Medical Academy, Faculty of clinical medicine , Tver , Russia
1972-1982	Ground school, specialized high school N 171, Main subjects physics and mathematics , Kiew, Ukraine

Professional experience:

Since Sept. 2004 -	Doctorand of Prof. Proff. h.c.(V.R.C) Dr.med Manfred Blank
Sept. 2003 - March 2004	Medical manager of Magscan GmbH, Essen , Germany
2000-2003	Leading researcher of SQUID AG , SQUID Int. AG , Essen , Germany
1995-1999	Researcher of National institute of Cardiology N.D. Strazesko , department of new diagnostic and Institute for Cybernetics of National Academy of science , department of medical cybernetics, Kiew , Ukraine
1992-1994	Physician-researcher of General clinical military hospital of Ukraine , department of cardiology and Center of medical engineering, Kiew , Ukraine
1991-1992	The 7-th Clinical Hospital, departments of general therapy and lungs diseases, physician- assistant Kiew, Ukraine
1989-1990	The 1-st Clinical Hospital, department of cardiology, physician-resident, Tver , Russia

Membership:

International Society of Electrocardiology;

Ukranian Society of cardiology;

Ukrainian Association of experts in medical computer science, statistics and biomedical engineering.